Activated Src-mediated reduction of gene expression is not totally dependent on Cas

Cas was originally cloned as a tyrosine phoshorylated protein in v-Crk- and v-Src-transformed cells [2] and Cas is reported to mediate transcriptional activation of the serum response element by Src [41]. Therefore we investigated the transcriptional change of these proteins in v-Src- or v-Crk-transformed rat 3Y1 cells [2] (Fig. 4, lanes 1–3). COL1A1, COL3A1, COL11A1, elastin, TSC-36, MARCKS, and caveolin-1 showed reduced expression with the transformation by v-Src (Fig. 4, lanes 1 and 2), but they showed slightly reduced expression with the transformation by v-Crk (Fig. 4, lanes 1 and 3). In contrast, the expression of heme oxygenase 1 was enhanced with the transformation by v-Src and was slightly up-regulated with the transformation by v-Crk (Fig. 4B, lanes 1–3). We could not detect the expression of periostin in these cells (data not shown).

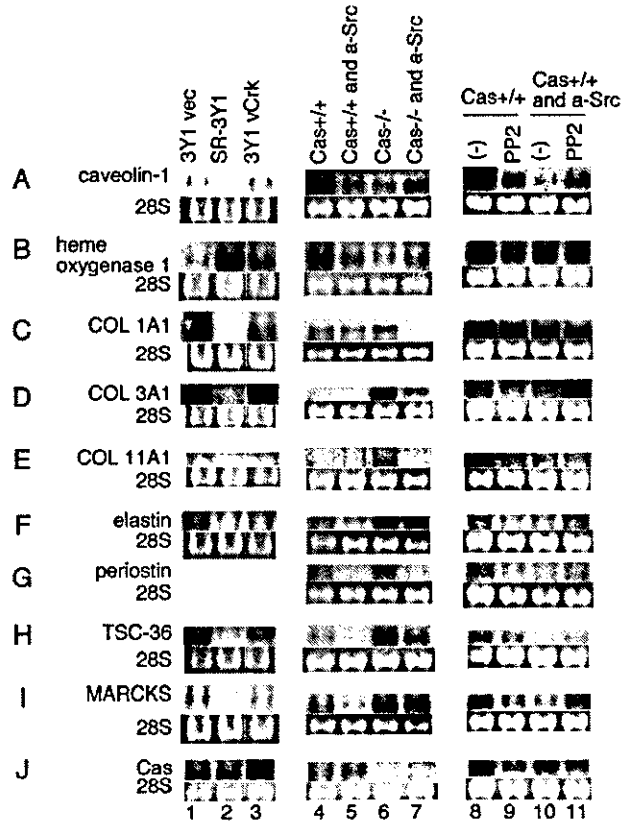

Fig. 4. Northern blots showing the regulation of target genes by activated Src expression. Total RNAs were harvested from 3Y1-vec (lane 1), SR-3Y1 (lane 2), 3Y1-vCrk (lane 3) [2], Cas +/+ cells (lane 4), Cas +/+ cells expressing a-Src (lane 5), Cas −/− cells (lane 6), Cas −/− cells expressing a-Src (lane 7) [21], Cas +/+ cells treated with DMSO as vehicle (lane 8), Cas +/+ cells treated with PP2, Src inhibitor (lane 9), Cas +/+ cells expressing a-Src treated with DMSO (lane 10), and Cas +/+ cells expressing a-Src treated with PP2 (lane 11). Ethidium bromide-stained 28S RNA levels are shown. The probes used are for caveolin-1 (A), heme oxygenase 1 (B), COL1A1 (C), COL3A1 (D), COL11A1 (E), elastin (F), periostin (G), TSC-36 (H), MARCKS (I), and Cas (J).

We next checked whether these Src-induced changes are dependent on Cas. RNAs were extracted from Cas −/− fibroblasts, Cas +/+ wild-type sibling-derived fibroblasts, Cas −/− fibroblasts transfected with a-Src, and Cas +/+ fibroblasts transfected with a-Src [21]. Both in Cas −/− cells and in Cas +/+ cells, the introduction of a-Src reduced the expression of the seven genes that were up-regulated in Cas −/− cells (Fig. 4C–I, lanes 4–7). However, COL3A1, elastin, TSC-36, and MARCKS showed higher expression in Cas −/− and a-Src cells than that of Cas +/+ cells (Fig. 4D, F, H, I, lanes 4–7). Caveolin-1 and heme oxygenase 1 showed reduced expression by a-Src in Cas +/+ cells, but their expression was increased by a-Src in Cas −/− cells (Fig. 4A, B, lanes 4–7).

To ascertain that the a-Src-induced change is dependent on tyrosine kinase activities, we treated the cells with 10 μM Src kinase inhibitor, PP2 (Wako) for 4 h. In Cas +/+ and a-Src-transformed cells, the expression was increased by PP2 (Fig. 4, lanes 10–11), confirming that a-Src-induced reduction of expression is kinase dependent. In contrast, untransformed Cas +/+ cells showed reduced expression when treated with PP2 (Fig. 4, lanes 8 and 9).

Discussion

In this report, we compared the expression profiles between Cas −/− fibroblasts and Cas-re-expressing fibroblasts. To avoid the clonal differences, we collected the polyclonal blasticidin-resistant clones. Among the genes differentially expressed in Cas −/− cells, nine genes (caveolin-1, heme oxygenase 1, COL1A1, COL3A1, COL11A1, elastin, periostin, TSC-36, and MARCKS) were selected for further analyses. These nine genes showed clear difference of expression not only between Cas −/− fibroblasts and Cas-re-expressing fibroblasts but also between Cas −/− fibroblasts and Cas +/+ fibroblasts.

Among the seven genes that are up-regulated in Cas −/− fibroblasts, six genes (COL1A1, COL3A1, COL11A1, elastin, periostin, and TSC-36) encode the extracellular matrix proteins and the other one, MARCKS, is known to regulate actin cytoskeleton [37]. Since Cas is known to be a signal transducer from integrin stimulation by ECM [15,16], the transcriptional reduction by Cas might be a result of negative feedback. Caveolin-1, which is up-regulated with expression of Cas, is also involved in integrin signaling [27,28] and is reported to reduce the Src kinase activity [42]. Although heme oxygenase 1 is not reported to be involved in integrin signaling, the oxidative stress that induces heme oxygenase 1 is reported to tyrosine phosphorylate Cas

[43]. These facts suggest that the nine genes are functionally related to Cas signaling.

In the case of caveolin-1, heme oxygenase 1, COL1A1, COL11A1, and elastin, the ΔSH3 mutant did not change the expression of them. This result could be attributed to the lower expression of the ΔSH3 mutant compared to other mutants, or the failure of this mutant to localize to focal adhesions [23]. However, it is also possible that signaling through the SH3 domain of Cas regulates the expression of these genes. Among the SH3 binding partners of Cas, CIZ is reported to regulate type I collagen [44,45]. The other binding partners such as C3G, PTP-PEST might play roles in this regulation. On the other hand, deletion of the substrate domain clearly abolished the change of expression of periostin (Fig. 3G). The signaling through the substrate domain is mediated by c-Crk that leads to DOCK180/Rac1/JNK pathway [17,18] and the expression of periostin might be regulated by this pathway. These results of the deletion study suggest multiple signaling pathways are involved in the gene regulation by Cas.

Reduction of expression of caveolin-1, COL1A1, and MARCKS [46–48] and enhancement of heme oxygenase-1 expression [49] by v-Src-induced transformation are reported. In this report, we added COL3A1, COL11A1, elastin, periostin, and TSC-36 as another down-regulated genes by v-Src (Fig. 4). However, TSC-36 is reported to be unchanged by v-Src transformation in NIH3T3 cells [34]. The discrepancy might be attributed to the difference of cell lines (we used 3Y1 cells and primary MEF) and suggests a limited role of TSC-36 in a-Src-mediated cell transformation. In addition, with the transformation by activated Src, the expression of heme oxygenase 1 showed reduction of expression in primary Cas +/+ MEFs (Fig. 4B, lanes 4 and 5) but enhancement in 3Y1 cells (Fig. 4B, lanes 1 and 2) and in CEFs [49] by v-Src. This differential regulation of heme oxygenase 1 by a-Src might suggest the irrelevancy of this gene in a-Src-mediated cell transformation.

In Cas −/− context, a-Src expression also reduced the expression of seven genes that were up-regulated in Cas −/− cells (Fig. 4C–J, lanes 6 and 7). Furthermore, the expression of the other two genes (caveolin-1 and heme oxygenase 1) that were down-regulated in Cas −/− cells were down-regulated or differentially regulated by a-Src expression. These facts indicate at least the existence of Cas-independent pathway that causes these regulations, or might suggest the possibility that Cas and a-Src independently regulate the expression of these genes, although the involvement of Cas in a-Src-mediated gene regulation was not excluded. In any case, we can at least say that Cas affects the expression of these genes that are regulated by a-Src-mediated transformation. The expression of COL3A1, elastin, TSC-36, and MARCKS in Cas −/− cells expressing a-Src is still higher than that in Cas +/+ cell transformed by a-Src and is even higher than that in Cas +/+ cells (Fig. 4D, F, H, I, lanes 4–7). Considering the fact that TSC-36 and MARCKS are reported to inhibit growth of cancer cells [35,39,40], the impaired transformation of Cas −/− MEF cells by v-Src [21] can be in part attributed to the overexpression of TSC-36 and MARCKS in these cells.

Since PP2 inhibition in Cas +/+ transformed by a-Src up-regulates the expression of caveolin-1, COL3A1, elastin, periostin, TSC-36, and MARCKS, the down-regulation by a-Src would be caused by the kinase activity of a-Src (Fig. 4, lanes 10 and 11). In contrast, PP2 reduced the expression in non-transformed Cas +/+ cells (Fig. 4, lanes 8 and 9). This reduction might be non-specific down-regulation including the expression of Cas (Fig. 4J, lanes 8 and 9). Otherwise, the role of non-transforming c-Src in the regulation of these genes might be different from that of a-Src and be related to the stronger down-regulation by ΔSB and RPLP mutants than by wild-type Cas (Fig. 3).

Overexpression of Cas in breast cancer was associated with tamoxifen resistance and with poor prognosis [50,51]. The transcriptional changes induced by Cas, especially those of TSC-36 and MARCKS, might contribute to the progression and invasion of carcinoma cells. Recently, another Cas family protein, HEF1/CasL, is reported to induce transcriptional change of matrix metalloproteinases and MLCK, p160Rock, which are believed to enhance cell migration and invasion [52]. On the other hand, TGF-β is known to regulate ECM proteins, periostin, and TSC-36 [25,31] and is implicated in fibrotic change in diseases. Considering the report that Cas is tyrosine phosphorylated by TGF-β stimulation [53], the results described here might suggest the possibility of the involvement of Cas in the deposition of ECM by TGF-β. Among the genes that showed differential expression in response to myocardial infarction included are collagens, caveolin family proteins, periostin, and ANP (atrial natriuretic peptide), which is reported to be mediated by Cas in cardiac cells [32,54]. The role of Cas and Cas-mediated transcriptional change in cancer progression, myocardial infarction, and other pathological processes would be a target for future study.

Acknowledgments

We thank Drs. Masaki Noda, Barbara E. Kream, and Kiyoshi Nose for generously providing probes. This work was in parts supported by Grants-in-Aids from the Ministry of Education, Science and Culture of Japan.

References

[1] R. Sakai, A. Iwamatsu, N. Hirano, S. Ogawa, T. Tanaka, J. Nishida, Y. Yazaki, H. Hirai, J. Biol. Chem. 269 (1994) 32740–32746.

[2] R. Sakai, A. Iwamatsu, N. Hirano, S. Ogawa, T. Tanaka, H. Mano, Y. Yazaki, H. Hirai, EMBO J. 13 (1994) 3748–3756.
[3] T. Nakamoto, R. Sakai, K. Ozawa, Y. Yazaki, H. Hirai, J. Biol. Chem. 271 (1996) 8959–8965.
[4] T. Gotoh, D. Cai, X. Tian, L.A. Feig, A. Lerner, J. Biol. Chem. 275 (2000) 30118–30123.
[5] A. Sakakibara, S. Hattori, J. Biol. Chem. 275 (2000) 6404–6464 (see also p. 6410).
[6] T.R. Polte, S.K. Hanks, Proc. Natl. Acad. Sci. USA 92 (1995) 10106–10678 (see also p. 10682).
[7] F. Liu, D.E. Hill, J. Chernoff, J. Biol. Chem. 271 (1996) 31290–31295.
[8] A.J. Garton, M.R. Burnham, A.H. Bouton, N.K. Tonks, Oncogene 15 (1997) 877–885.
[9] K.H. Kirsch, M.M. Georgescu, H. Hanafusa, J. Biol. Chem. 273 (1998) 25673–25679.
[10] K.H. Kirsch, M.M. Georgescu, S. Ishimaru, H. Hanafusa, Proc. Natl. Acad. Sci. USA 96 (1999) 6211–6216.
[11] T. Nakamoto, T. Yamagata, R. Sakai, S. Ogawa, H. Honda, H. Ueno, N. Hirano, Y. Yazaki, H. Hirai, Mol. Cell. Biol. 20 (2000) 1649–1658.
[12] D.D. Schlaepfer, M.A. Broome, T. Hunter, Mol. Cell. Biol. 17 (1997) 1702–1713.
[13] J. Yi, S. Kloeker, C.C. Jensen, S. Bockholt, H. Honda, H. Hirai, M.C. Beckerle, J. Biol. Chem. (2002).
[14] E. Li, D.G. Stupack, S.L. Brown, R. Klemke, D.D. Schlaepfer, G.R. Nemerow, J. Biol. Chem. 275 (2000) 14729–14735.
[15] Y. Nojima, N. Morino, T. Mimura, K. Hamasaki, H. Furuya, R. Sakai, T. Sato, K. Tachibana, C. Morimoto, Y. Yazaki, H. Hirai, J. Biol. Chem. 270 (1995) 15398–15402.
[16] K. Vuori, E. Ruoslahti, J. Biol. Chem. 270 (1995) 22259–22262.
[17] F. Dolfi, M. Garcia-Guzman, M. Ojaniemi, H. Nakamura, M. Matsuda, K. Vuori, Proc. Natl. Acad. Sci. USA 95 (1998) 15394–15399.
[18] E. Kiyokawa, Y. Hashimoto, S. Kobayashi, H. Sugimura, T. Kurata, M. Matsuda, Genes Dev. 12 (1998) 3331–3336.
[19] L.A. Cary, D.C. Han, T.R. Polte, S.K. Hanks, J.L. Guan, J. Cell. Biol. 140 (1998) 211–221.
[20] R.L. Klemke, J. Leng, R. Molander, P.C. Brooks, K. Vuori, D.A. Cheresh, J. Cell. Biol. 140 (1998) 961–972.
[21] H. Honda, H. Oda, T. Nakamoto, Z. Honda, R. Sakai, T. Suzuki, T. Saito, K. Nakamura, K. Nakao, T. Ishikawa, M. Katsuki, Y. Yazaki, H. Hirai, Nat. Genet. 19 (1998) 361–365.
[22] H. Honda, T. Nakamoto, R. Sakai, H. Hirai, Biochem. Biophys. Res. Commun. 262 (1999) 25–30.
[23] T. Nakamoto, R. Sakai, H. Honda, S. Ogawa, H. Ueno, T. Suzuki, S. Aizawa, Y. Yazaki, H. Hirai, Mol. Cell. Biol. 17 (1997) 3884–3897.
[24] P. Chomczynski, N. Sacchi, Anal. Biochem. 162 (1987) 156–159.
[25] M. Shibanuma, J. Mashimo, A. Mita, T. Kuroki, K. Nose, Eur. J. Biochem. 217 (1993) 13–19.
[26] E.J. Smart, G.A. Graf, M.A. McNiven, W.C. Sessa, J.A. Engelman, P.E. Scherer, T. Okamoto, M.P. Lisanti, Mol. Cell. Biol. 19 (1999) 7289–7304.
[27] K.K. Wary, F. Mainiero, S.J. Isakoff, E.E. Marcantonio, F.G. Giancotti, Cell 87 (1996) 733–743.
[28] K.K. Wary, A. Mariotti, C. Zurzolo, F.G. Giancotti, Cell 94 (1998) 625–634.
[29] M.D. Maines, Annu. Rev. Pharmacol. Toxicol. 37 (1997) 517–554.
[30] S. Takeshita, R. Kikuno, K. Tezuka, E. Amann, Biochem. J. 294 (Pt 1) (1993) 271–278.
[31] K. Horiuchi, N. Amizuka, S. Takeshita, H. Takamatsu, M. Katsuura, H. Ozawa, Y. Toyama, L.F. Bonewald, A. Kudo, J. Bone Miner. Res. 14 (1999) 1239–1249.
[32] L.W. Stanton, L.J. Garrard, D. Damm, B.L. Garrick, A. Lam, A.M. Kapoun, Q. Zheng, A.A. Protter, G.F. Schreiner, R.T. White, Circ. Res. 86 (2000) 939–945.
[33] A. Kruzynska-Frejtag, M. Machnicki, R. Rogers, R.R. Markwald, S.J. Conway, Mech. Dev. 103 (2001) 183–188.
[34] J. Mashimo, R. Maniwa, H. Sugino, K. Nose, Cancer Lett. 113 (1997) 213–219.
[35] K. Sumitomo, A. Kurisaki, N. Yamakawa, K. Tsuchida, E. Shimizu, S. Sone, H. Sugino, Cancer Lett. 155 (2000) 37–46.
[36] I.M. Johnston, H.J. Spence, J.N. Winnie, L. McGarry, J.K. Vass, L. Meagher, G. Stapleton, B.W. Ozanne, Oncogene 19 (2000) 5348–5358.
[37] A. Arbuzova, A.A. Schmitz, G. Vergeres, Biochem. J. 362 (2002) 1–12.
[38] S. Manenti, F. Malecaze, J.M. Darbon, FEBS Lett. 419 (1997) 95–98.
[39] G. Brooks, S.F. Brooks, M.W. Goss, Carcinogenesis 17 (1996) 683–689.
[40] S. Manenti, F. Malecaze, H. Chap, J.M. Darbon, Cancer Res. 58 (1998) 1429–1434.
[41] Y. Hakak, G.S. Martin, Mol. Cell. Biol. 19 (1999) 6953–6962.
[42] S. Li, J. Couet, M.P. Lisanti, J. Biol. Chem. 271 (1996) 29182–29190.
[43] M. Yoshizumi, J. Abe, J. Haendeler, Q. Huang, B.C. Berk, J. Biol. Chem. 275 (2000) 11706–11712.
[44] K. Furuya, T. Nakamoto, Z.J. Shen, K. Tsuji, A. Nifuji, H. Hirai, M. Noda, Exp. Cell Res. 261 (2000) 329–335.
[45] P. Thunyakitpisal, M. Alvarez, K. Tokunaga, J.E. Onyia, J. Hock, N. Ohashi, H. Feister, S.J. Rhodes, J.P. Bidwell, J. Bone Miner. Res. 16 (2001) 10–23.
[46] J.A. Engelman, X.L. Zhang, B. Razani, R.G. Pestell, M.P. Lisanti, J. Biol. Chem. 274 (1999) 32333–32341.
[47] B.J. Frankfort, I.H. Gelman, Biochem. Biophys. Res. Commun. 206 (1995) 916–926.
[48] C.K. Joseph, S.A. Qureshi, D.J. Wallace, D.A. Foster, J. Biol. Chem. 267 (1992) 1327–1330.
[49] J.G. Hoey, J. Summy, D.C. Flynn, Cell. Signal. 12 (2000) 691–701.
[50] A. Brinkman, S. van der Flier, E.M. Kok, L.C. Dorssers, J. Natl. Cancer Inst. 92 (2000) 112–120.
[51] S. van der Flier, A. Brinkman, M.P. Look, E.M. Kok, M.E. Meijer-van Gelder, J.G. Klijn, L.C. Dorssers, J.A. Foekens, J. Natl. Cancer Inst. 92 (2000) 120–127.
[52] S.J. Fashena, M.B. Einarson, G.M. O'Neill, C. Patriotis, E.A. Golemis, J. Cell Sci. 115 (2002) 99–111.
[53] M.C. Riedy, M.C. Brown, C.J. Molloy, C.E. Turner, Exp. Cell. Res. 251 (1999) 194–202.
[54] B. Kovacic-Milivojevic, F. Roediger, E.A. Almeida, C.H. Damsky, D.G. Gardner, D. Ilic, Mol. Biol. Cell. 12 (2001) 2290–2307.

THE JOURNAL OF BIOLOGICAL CHEMISTRY
Vol. 277, No. 30, Issue of July 26, pp. 27265–27272, 2002
Printed in U.S.A.

Differential Regulation of Cell Migration, Actin Stress Fiber Organization, and Cell Transformation by Functional Domains of Crk-associated Substrate*

Received for publication, March 29, 2002
Published, JBC Papers in Press, May 14, 2002, DOI 10.1074/jbc.M203063200

Jinhong Huang‡§, Hiroko Hamasaki‡, Tetsuya Nakamoto¶, Hiroaki Honda¶, Hisamaru Hirai¶, Masaki Saito‖, Tsuyoshi Takato§, and Ryuichi Sakai‡**

From the ‡Cancer Signal Transduction Project, National Cancer Center Research Institute, 5-1-1 Tsukiji, Chuo-ku, Tokyo 104-0045, the §Department of Oral and Maxillofacial Surgery and ¶Department of Hematology and Oncology, University of Tokyo, 7-3-1 Hongo, Bunkyo-ku, Tokyo 113-8655, and the ‖Department of Oncology and Pharmacodynamics, Meiji Pharmaceutical University, 2-522-1 Noshino, Kiyose-shi, Tokyo 20-4-8588, Japan

The Crk-associated substrate (Cas) is a unique docking protein that possesses a repetitive stretch of tyrosine-containing motifs and an Src homology 3 (SH3) domain. Embryonic fibroblasts lacking Cas demonstrated resistance to Src-induced transformation along with impaired actin bundling and cell motility, indicating critical roles of Cas in actin cytoskeleton organization, cell migration, and oncogenesis. To gain further insight into roles of each domain of Cas in these processes, a compensation assay was performed by expressing a series of Cas mutants in Cas-deficient fibroblasts. The results showed that motifs containing YDxP were indispensable for actin cytoskeleton organization and cell migration, suggesting that CrkII-mediated signaling regulates these biological processes. The C-terminal Src-binding domain played essential roles in cell migration and membrane localization of Cas, although it was dispensable in the organization of actin stress fibers. Furthermore, the Src-binding domain was also a prerequisite for Src transformation possibly, because of its crucial role in the phosphorylation of Cas during transformation. Overall, differential uses of the Cas domains in individual biological processes were demonstrated.

Cas[1] docking protein was initially identified and cloned as a major phosphotyrosine-containing protein in cells transformed by v-*src* and v-*crk* oncogenes (1, 2). It has a structure with a number of protein-protein interaction domains, including an N-terminal Src homology 3 (SH3) domain, a substrate domain (SD) that consists of a cluster of YxxP motifs (one YLVP, four YQxPs, nine YDxPs, and one YAVP), and a C-terminal Src-binding domain containing motifs YDYV (amino acids 762–765) and RPLPSPP (2). The substrate domain offers docking sites for several molecules including adaptor proteins Crk, Nck, and an inositol 5′-phosphatase, SHIP2 (SH2-containing inositol 5′-phosphatase), through their SH2 domains in a phosphorylation dependent manner (3–5). Motifs RPLPSPP and YDYV in the SB domain serve as direct binding sites for SH3 and SH2 domains of Src family kinases, respectively (6). The SH3 domain could bind proline-rich sequences of various signaling molecules such as focal adhesion kinase (FAK) (7), guanine nucleotide exchange factor C3G (8), and tyrosine phosphatase PTP-PEST (9).

As for biological functions, Cas is phosphorylated at tyrosines in normal cells following activation of integrins (10, 11) and stimulation with bioactive lipid lysophosphatidic acid (LPA) and mitogenic neuropeptides such as bombesin (12) directly by Src family kinases (6, 13–16). Phosphorylated Cas is localized to focal adhesions where it appears to recruit numerous binding partners such as FAK (17), Crk (18), and PTP-PEST (19) to participate in the signaling of cell adhesion and migration. On the other hand, Cas was originally found as a putative substrate of the v-Src kinase and a binding target for the SH2 domain of v-Crk, implying that phosphorylation of Cas is closely associated with retroviral transformation. Earlier study using the antisense Cas mRNA also supported the idea that Cas is a positive regulator of cell transformation (20). It was finally confirmed by the fact that mouse embryonic fibroblasts lacking Cas were resistant to Src induced transformation. Cas-deficient mouse embryonic fibroblasts also showed impaired actin bundling and cell migration. These phenotypes were restored after re-expression of Cas, suggesting that Cas plays essential roles in the signal transduction of actin cytoskeleton organization, cell migration and transformation (21, 22). An open question now is how each functional domain of Cas is utilized during the specific biological events mentioned above. The answer will be important for the understanding of how this molecule serves as a docking port for many distinct signal inputs and how it ultimately contributes to generation of appropriate cellular responses.

Therefore, we investigated the roles of each domain of Cas in actin stress fiber organization, cell migration, and Src transformation by establishing Cas−/− fibroblast lines stably expressing a series of systemic mutants of each protein-binding domain of Cas. The capability of each mutant to rescue actin stress fiber organization, cell migration, and Src transformation was analyzed to identify essential domains responsible for each biological process. It was demonstrated that Cas participates in multifold biological processes by utilizing many protein-binding sites in an event-specific manner.

* This work was supported in part by a scholarship from the HonJo International Scholarship Foundation of Japan. The costs of publication of this article were defrayed in part by the payment of page charges. This article must therefore be hereby marked "*advertisement*" in accordance with 18 U.S.C. Section 1734 solely to indicate this fact.

** To whom correspondence should be addressed: Cancer Signal Transduction Project, National Cancer Center Research Institute, 5-1-1 Tsukiji, Chuo-ku, Tokyo 104-0045, Japan. Tel.: 81-3-3542-2511, Ext. 4701; Fax: 81-3-3543-2181; E-mail: rsakai@gan2.res.ncc.go.jp.

[1] The abbreviations used are: Cas, Crk-associated substrate; Cas-FL, full-length Cas; SH3, Src homology 3 domain; SH2, Src homology 2 domain; FAK, focal adhesion kinase; C3G, Crk SH3 guanine nucleotide-releasing factor; LPA, lysophosphatidic acid; FITC, fluorescein isothiocyanate; SD, substrate domain; SB, Src-binding domain; PTP, protein tyrosine phosphatase; DMEM, Dulbecco's modified Eagle's medium; FBS, fetal bovine serum; PBS, phosphate-buffered saline.

EXPERIMENTAL PROCEDURES

Stable Expression of Cas Mutants In Cas−/− and Cas−/−Src Fibroblasts—The short form of rat Cas cDNA (encoding an 874-amino acid product), with deletions of the SH3 domain (ΔSH3), the SB domain (ΔSB), the substrate domain (ΔSD), motifs YQxP (ΔYQxP) and YDxP (ΔYDxP), the SH3 and SB domains (ΔSH3·SB), and both the SH3 domain and YDxP motifs (ΔSH3·YDxP), or mutation of Y762 (Y762F), RPLP (RLGS), Y762, and RPLP (RLGS-Y762F), were HA-tagged and constructed, respectively, into expression vector pSSRα-bsr, which contains an SRα promoter and a blasticidin-resistance gene as described previously (6). The resulting plasmids were transfected into mouse embryonic Cas-deficient fibroblasts (Cas−/−) or Cas−/−Src fibroblasts (Cas-deficient fibroblasts stably expressing 527F-c-Src, an activated form of c-Src) (21). Transfection was performed using Fugene™ 6 transfection reagent (Roche Molecular Biochemicals) according to the manufacturer's instruction. In detail, 6×10^5 Cas−/− fibroblasts were plated into 10-cm dish and cultured overnight. 12 μl of Fugene reagent was incubated with serum-free medium for 5 min and then mixed with 6 μg of DNA and co-incubated for 15 min before being introduced into cells. Transfected cells were subjected to blasticidin selection (5 μg/ml) for Cas−/− cells or blasticidin (5 μg/ml) and puromycin (1 μg/ml) double selection for Cas−/−Src cells after 48 h as described previously (21). Colonies formed 2 weeks later were then picked up, expanded, and subjected to Western blot screening for expression of Cas mutants.

Antibodies and Reagents—Antibodies against HA or CrkII were from Santa Cruz Biotechnology, anti-phosphotyrosine antibody 4G10 was from Upstate Biotechnology, and polyclonal antibody αCas2 against Cas was used as described previously (2). Monoclonal antibody 2-17 against Src was from Microbiological Associates. FITC-labeled phalloidin was purchased from Sigma, and FITC-conjugated anti-rabbit antibody was from Santa Cruz Biotechnology. Bovine plasma fibronectin was purchased from Sigma. Y-27632 dihydrochloride was from Tocris Cookson Ltd. (Avonmouth, Bristol, UK), and LPA was from Sigma.

Immunoblotting and Immunoprecipitation—Protein extraction and Western blotting analysis were performed as described (6). Briefly, cells were lysed in 1% Triton X-100 buffer (50 mM Hepes, 150 mM NaCl, 10% glycerol, 1% Triton X-100, 1.5 mM $MgCl_2$, 1 mM EGTA, 100 mM NaF, 1 mM Na_3VO_4, 10 μg/ml aprotinin, 10 μg/ml leupeptin, 1 mM phenylmethylsulfonyl fluoride). Protein aliquots were separated by SDS-PAGE and probed with antibodies diluted 1:2000. For immunoprecipitation, 500 μg of protein was mixed with 1 μg of anti-HA antibody or 1 μg of αCas2 and incubated for 1 h on ice. Then samples were rotated with protein A-Sepharose (Sigma) for 1 h at 4 °C, and beads were washed four times with 1% Trixon X-100 buffer and boiled in sample buffer before being subjected to SDS-PAGE analysis.

Immunofluorescence—Immunofluorescence was performed essentially as described previously (23). 3×10^4 cells were plated into each well of an 8-well chamber slide and allowed to grow for 48 h in DMEM with 10% FBS at 37 °C with 5% CO_2. Cells were then fixed with 4% paraformaldehyde/PBS for 1 h, washed three times with PBS, and incubated with FITC-phalloidin (50 μg/ml) to stain actin filaments for 1 h on ice. To analyze the effects of Y-27632 and LPA on actin stress fiber formation, cells were serum-starved for 24 h before incubation in serum-free medium containing Y-27632 (10 μM) or LPA (10 μM) respectively. After 1 h, cells were fixed and stained by FITC-labeled phalloidin. For staining, Cas mutants were washed three times with PBS after fixation, and then cells were permeabilized with 0.3% Triton X-100 buffer (50 mM Hepes, 150 mM NaCl 10% glycerol, 0.3% Triton X-100, 1.5 mM $MgCl_2$, 1 mM EGTA, 100 mM NaF, 1 mM Na_3VO_4, 10 μg/ml aprotinin, 10 μg/ml leupeptin, 1 mM phenylmethylsulfonyl fluoride) for 5 min before incubation with the primary antibody. The primary antibody αCas2 was used at 10 ng/μl for 2 h, and secondary antibody FITC-conjugated anti-rabbit was used at 1:40 for 1 h. After cells were washed three times by PBS, cover glasses were mounted using mounting liquid (Entellan; Merck). Cells were then visualized by an Olympus fluorescence microscope, and photographs were taken at the original magnification of 200×.

Wound-healing Assay—Wound-healing assay was performed according to a method used previously (22). Briefly, cells were first grown to confluence in plastic culture dishes, and a wound was made in the cell monolayer using a sterile micropipette tip. Then cells were cultured at 37 °C with 5% CO_2 in DMEM containing 10% FBS after being washed three times with PBS. Cell movement was assessed 24 h after wounding from photographs taken under the microscope with a 40× objective. The percentage of reduced distance between the nuclei of cells moving forward 24 h later relative to the distance between two rims in the cleared field at the beginning was taken as the index.

Cell Migration Assay—Migration of all the cell lines was also analyzed using a Boyden chamber cell migration assay with some modification (22). In detail, polyvinylpyrrolidine-free polycarbonate filters with a pore size of 8 μm (Neuroprobe) were coated for 30 min with fibronectin (10 μg/ml) in DMEM containing 10% FBS. The coated filters were then dried and placed over the lower well of a Boyden chamber, which was then filled with 1.28 ml of DMEM containing 10% FBS. After being detached from the culture dishes by exposure to 5% trypsin-EDTA, 1.5×10^5 cells in 0.56 ml of DMEM containing 10% FBS were added to the upper well. The chamber was then placed in a humidified incubator containing 5% CO_2 for 4 h at 37 °C. Cells on the membrane that had migrated through the filter were fixed in methanol for 30 min, washed with PBS, and then exposed to Giemsa staining for 15 s. After three washes with PBS, the filter was mounted on a glass slide. The side of the filter to which cells had been added was scraped. The number of migrated cells was counted from photographs taken of at least eight fields at a magnification of 200× under the microscope.

Soft Agar Colony Formation Assay—Soft agar colony formation assay was performed as described previously (21). Briefly, 10^5 trypsinized cells were resuspended in DMEM containing 10% FBS and 0.4% SeaPlaque GTG agarose (Bioproducts) and poured onto bottom agar containing 10% FBS and 0.53% agarose in 6-cm culture dishes. Then cells were incubated at 37 °C with 5% CO_2. After 14 days, colonies containing more than 5 cells were counted under the microscope with a 100× objective.

RESULTS

Roles of Each Domain or Motif of Cas in Actin Stress Fiber Organization—The short form of Cas cDNA encoding an 874-amino acid product was used for construction of a series of Cas mutants as described previously (6). Each Cas deletion mutant along with full-length Cas (CasFL) were HA-tagged and subcloned into vector pSSRα-bsr, which contains an SRα promoter. Cas mutants that lacks the SH3 domain, the substrate domain, YQxP motifs, YDxP motifs, or the Src-binding domain were defined as ΔSH3, ΔSD, ΔYQxP, ΔYDxP, and ΔSB, respectively. Cas cDNA that mutated at RPLP, Y762, or both in the C-terminal Src-binding domain were named RLGS, Y762F, and RLGS-Y762F, respectively (Fig. 1*A*). Multiple clones expressing individual Cas mutants in Cas−/− fibroblasts (Cas-deficient fibroblasts) were selected using immunoblotting by antibodies against Cas and HA (Fig. 1*B*). We failed to establish Cas−/− fibroblast expressing ΔYQxP to the level comparable with other mutants, although we tried several independent transfections.

It was confirmed by phalloidin staining that actin stress fibers were totally disrupted in Cas−/− fibroblasts, whereas they were restored by expressing CasFL as already reported (Fig. 2, *a* and *b*). No detectable actin stress fibers were formed in cell lines expressing ΔSD or ΔYDxP similar to the original Cas−/− fibroblasts, indicating that YDxP motifs located in the center of the SD domain were indispensable for the signal transduction of actin stress fiber organization (Fig. 2, *d* and *f*). In contrast, a series of mutants, ΔSH3, ΔYQxP, ΔSB, RLGS, Y762F, and RLGS-Y762F, could reorganize actin stress fibers in Cas−/− cells at least to the same level as CasFL (Fig. 2, *c*, *e*, and *g–j*), indicating that these domains or motifs are not required for actin stress fiber formation.

The fact that two of major protein-binding domains of Cas, the SH3 and Src-binding domains, were dispensable, raised a new question as to whether these domains are redundant for actin stress fiber formation (*i.e.* whether only one of these domains is required) or whether none of these domains is required for this event. To answer this question, a Cas mutant with deletion of both the SH3 and SB domains (ΔSH3·SB) was constructed and stably expressed into Cas−/− fibroblasts (Fig. 1). Phalloidin staining showed that actin stress fibers were significantly reorganized in Cas−/− cells expressing ΔSH3·SB (Fig. 2*k*). It was suggested that YDxP motifs were involved in the signal transduction of actin organization independently of other domains of Cas. Additionally, it was noticed that the

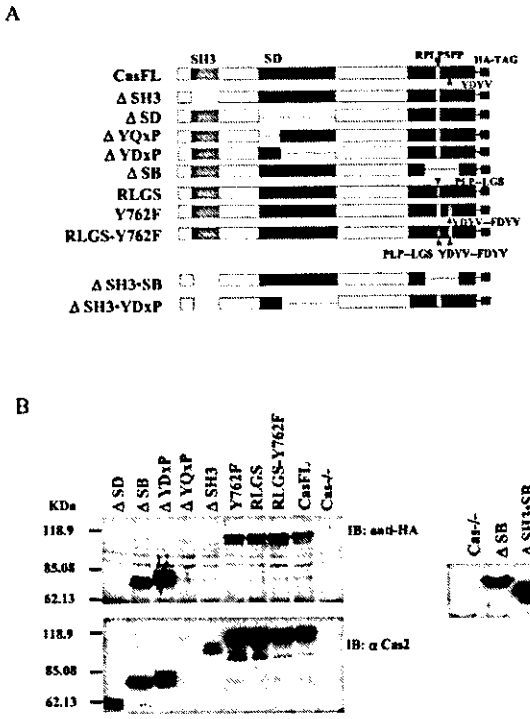

FIG. 1. **Establishment of cell lines stably expressing series of Cas mutants in Cas−/− fibroblasts.** *A*, HA-tagged Cas mutational constructs. *CasFL*, Cas full-length; *ΔSD*, the substrate domain deletion; *ΔYQxP*, YQxP motif deletion; *ΔYDxP*, YDxP motif deletion; *ΔSH3*, the SH3 domain deletion; *ΔSB*, the Src-binding domain deletion; *Y762F*, YDYV mutated to FDYV; *RLGS*, RPLP mutated to RLGS; *RLGS-Y762F*, RPLP and YDYV motifs, double mutation; *ΔSH3-SB*, deletion of SH3 and SB domains; *ΔSH3-YDxP*, deletion of the SH3 domain and YDxP motifs. *B*, a series of cell lines stably expressing ΔSD, ΔSB, ΔYDxP, ΔYQxP, ΔSH3, Y762F, RLGS, and RLGS-Y762F mutants, CasFL (*left panel*), or ΔSH3-SB (*right panel*) in Cas−/− fibroblasts. Expression of mutant protein was confirmed by antibody αCas2 and antibody against HA.

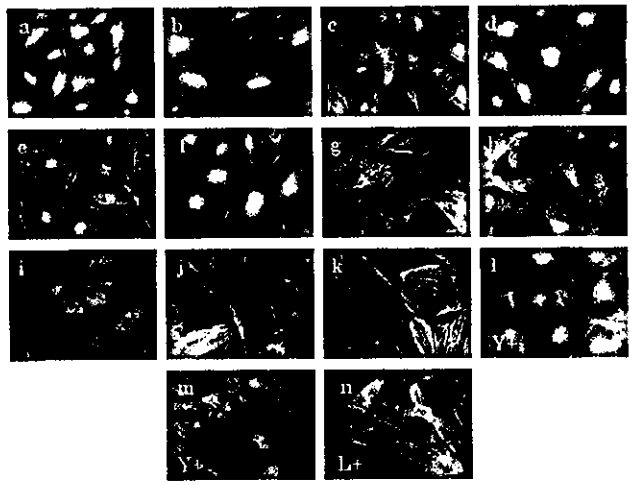

FIG. 2. **Rescue of actin stress fiber organization by cell lines stably expressing a series of mutants of each domain of Cas.** Actin filaments were stained by FITC-labeled phalloidin in cell lines stably expressing a series of Cas mutants. Cells allowed to grow for 48 h in DMEM with 10% FBS were fixed and incubated with FITC-labeled phalloidin (Sigma) for 1 h on ice and visualized by an Olympus fluorescence microscope with a 200× objective. *a–k*, actin stress fibers reorganized in Cas−/−, CasFL, and all of the cell lines expressing Cas mutants. *a*, Cas−/− cells; *b*, CasFL; *c*, ΔSH3; *d*, ΔSD; *e*, ΔYQxP; *f*, ΔYDxP; *g*, ΔSB; *h*, –Y762F; *i*, RLGS; *j*, RLGS-Y762F; *k*, ΔSH3-SB. *l–n*, effects of Y-27632 and LPA on actin stress fiber formation. Cells were serum-starved for 24 h before incubated in serum-free medium containing Y-27632 (10 μM) or LPA (10 μM), respectively. Cells were then fixed and stained for 1 h by FITC-labeled phalloidin. *l*, CasFL with Y-27632; *m*, RLGS-Y762F with Y-27632; *n*, Cas−/− with LPA.

amount of actin stress fibers formed by expressing ΔSH3, RLGS-Y762F, ΔSB, or ΔSH3-SB mutant (Fig. 2, *c*, *j*, *g*, and *k*, respectively) appeared to be rather excessive compared with that formed by expressing CasFL (Fig. 2*b*), although the mechanism was not clear. Actin stress fibers restored by CasFL or RLGS-Y762F were completely disrupted by Y-27632 (24), an inhibitor of the Rho-associated kinase (p160ROK) (Fig. 2, *l* and *m*), suggesting that the original Rho-ROK pathway was utilized in these restoration processes. LPA, a Rho family activator, could induce the formation of actin stress fibers in Cas−/− fibroblasts (Fig. 2*n*), indicating that LPA-mediated signal activation involves either downstream or alternative pathways of Cas in actin stress fiber organization.

Results of Wound-healing Assay and Boyden Chamber Cell Migration Assay—To investigate domain functions of Cas in the signal transduction of cell migration, wound-healing assay and Boyden chamber cell migration assay were performed. In a wound-healing assay, cell motility was judged from the reduction of the gap 24 h after the wound was made. Consistent with the previous report, original Cas−/− fibroblasts exhibited only about 17.3% reduction, whereas expression of CasFL showed complete restoration of cell mobility, causing 97.4% healing of the wound (22). Expression of Y762F showed almost complete restoration of the gap (95.6%), and ΔSH3 mutants resulted in 45.7% reduction of the wound (Fig. 3) possibly because the expression level of ΔSH3 is lower than others. No significant improvement (about 20% reduction of the gap) of cell migration was obtained by expressing ΔSD, ΔYDxP, ΔSB, RLGS, or RLGS-Y762F mutants compared with Cas−/− fibroblasts, indicating an essential role for YDxP motifs in the SD domain and RPLP motif in the SB domain in cell migration.

In a Boyden chamber assay, cell mobility was analyzed by counting the number of cells migrating through pores of the filter coated with fibronectin. As shown in Fig. 4, as few as ~8 cells/field could migrate through the filter by fibroblasts lacking Cas protein, whereas 70 cells/field could move through the filter by expression of CasFL. Y762F or ΔSH3 mutants gained cell motility of 70 or 40 cells/field, respectively, showing that these domains are not crucial for cell migration by this assay. Expression of ΔSD, ΔYDxP, ΔSB, RLGS, or RLGS-Y762F mutants, however, failed to improve the cell motility of Cas−/− fibroblasts by Boyden chamber assay. As expected, ΔSH3-SB failed to restore the cell mobility impaired in Cas−/− fibroblasts in both the wound-healing and Boyden chamber assays (Figs. 3*B* and 4). Because we failed to get clones to express enough of the ΔYQxP mutant (Fig. 1*B*), it could not be concluded that YQxP motifs are dispensable for cell migration from the result that cell mobility was not detectably rescued by ΔYQxP (Figs. 3 and 4), although the same amount of the mutant protein did rescue actin stress fiber formation.

Direct association of Cas and Crk was indicated both by screening of a synthetic peptide library and an *in vitro* binding assay (6, 25). Previous results showed that CrkII served as signal effectors in actin cytoskeleton organization and cell migration (18). To elucidate the roles of YDxP motifs expressed in Cas−/− fibroblasts in actin stress fiber organization and cell migration, the association of Cas with CrkII was investigated by immunoprecipitation. It was confirmed that CasFL and mutants RLGS, Y762F, and RLGS-Y762F, but not ΔYDxP, were co-precipitated with CrkII (Fig. 5), implicating a role of CrkII-mediated signaling through the YDxP motifs of Cas in cell migration and actin stress fibers organization.

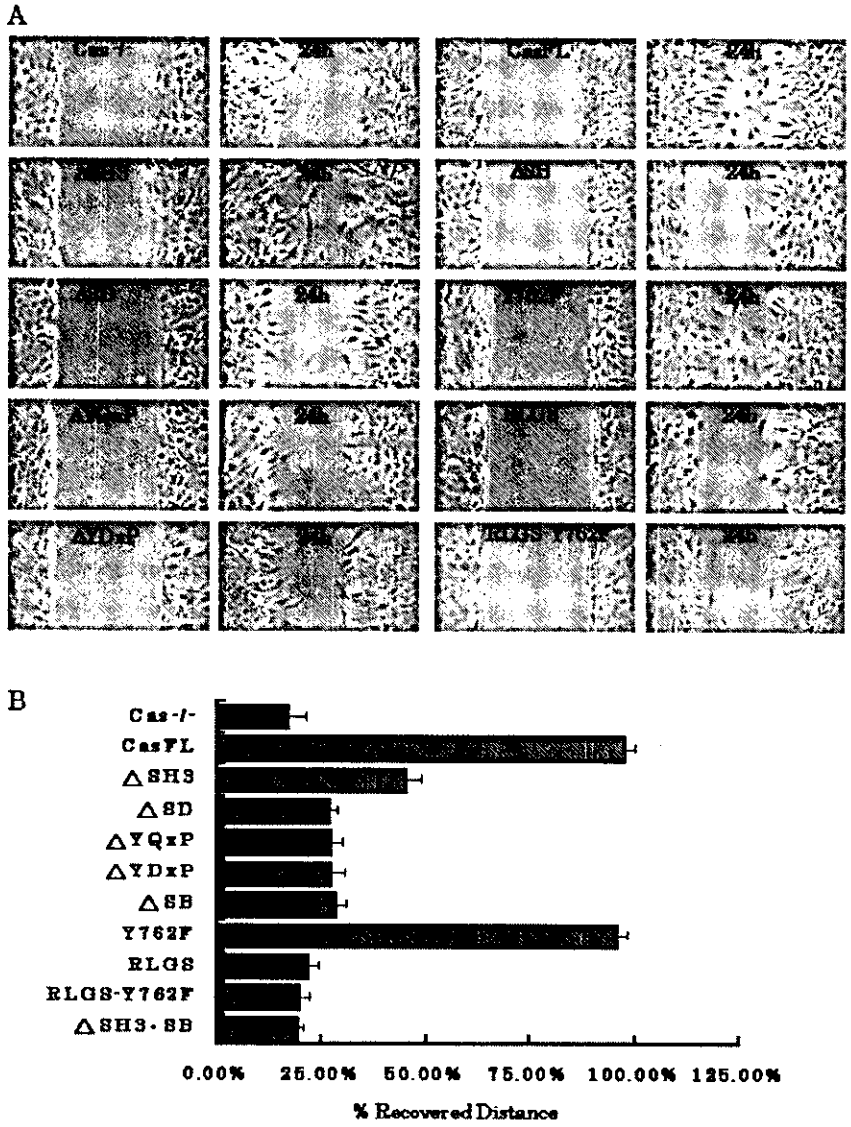

FIG. 3. **Restoration of cell motility by various Cas mutants in wound-healing assay.** *A*, photographs of cells 24 h after wounding. Wounds were made on a monolayer of cells grown to confluence and then incubated for 24 h at 37 °C with 5% CO_2 in DMEM containing 10% FBS after washing by PBS. Photographs were taken at the beginning and 24 h later under a microscope with an objective of 40×. *B*, quantitative analysis of the percentage of gap reduction by various Cas mutants (*error bars* show the standard deviation). The percentage of reduced distance between nuclei of cells moving forward 24 h after wounding relative to the distance between two rims at the beginning was taken as the index. Results presented here are representative mean values of four times experiments with three independent clones of each cell line.

Subcellular Localization of Cas Mutants—As the subcellular localization of Cas is closely associated with its role in signal transduction, localization of CasFL, ΔYDxP, and RLGS-Y762F in cell lines established was investigated by immunocytostaining. In CasFL (Fig. 6*b*)- and ΔYDxP (Fig. 6*c*)-expressing cells, several dense areas of staining appeared around the plasma membrane, showing the membrane-located fraction of Cas. This kind of localization was not observed in RLGS-Y762F mutant-expressing cells, indicating that RLGS-Y762F mutant is not able to localize to the cell membrane and exhibits cytoplasmic distribution (Fig. 6*d*). Focal adhesions were also investigated by vinculin staining in the cell lines mentioned above, and no significant difference in the number was observed just as reported for Cas −/− cells (21).

The SB Domain Plays a Central Role in Transformation by Src—Similar series of systemic mutants of each domain of Cas were stably introduced into Cas−/−Src cells, Cas−/− fibroblasts expressing activated c-Src (527F-c-Src) (21) (Fig. 7*A*). Anchorage-independent growth during Src transformation was examined by a soft agar colony formation assay. As shown by the results in Fig. 7*B*, almost no colonies were formed by Cas-deficient fibroblasts even in the presence of activated Src, but a considerable number of colonies were formed by cells expressing CasFL, as reported previously (21). Expression of ΔSH3, ΔYDxP, or Y762F was also able to restore colony formation capability, suggesting that motifs YDxP and Y762 and domain SH3 are dispensable for Src transformation. In contrast, similar to Cas−/− fibroblasts, ΔSB, RLGS, and RLGS-Y762F mutants failed to recover colonies formation as the result of several experiments. It was shown that the SB domain of Cas is critical for anchorage-independent growth by activated Src. As we failed to get clones to express ΔSD or ΔYQxP in Cas−/−Src cells even after many trials, the role of YQxP motifs in transformation was not clear.

To know whether the SB domain participates in this process by itself, Cas containing deletion of both the YDxP motifs and the SH3 domain (ΔSH3·YDxP) was stably expressed in Cas−/−Src fibroblasts (Fig. 7*A*). It was shown that comparable numbers of colonies were formed by ΔSH3·YDxP, ΔSH3, and ΔYDxP (Fig. 7*B*), suggesting that both the SH3 domain and YDxP motifs of Cas are dispensable for soft agar colony formation. The SB domain that remains in the ΔSH3·YDxP mutant might be responsible for the signal transduction of anchorage-independent growth in Src transformed cells.

Phosphorylation of Cas Mutants Re-expressed in Cas−/− or Cas−/−Src Fibroblast—To further explore the mechanisms

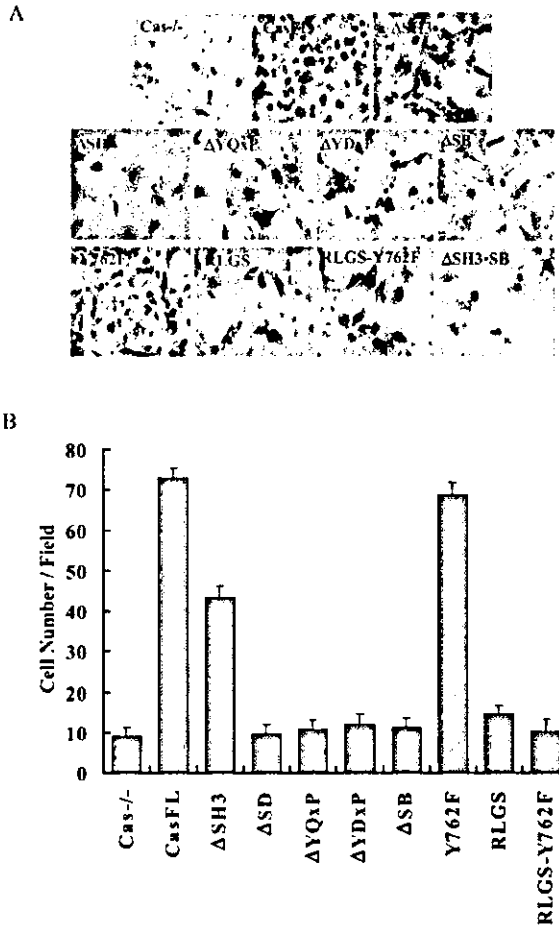

FIG. 4. **Boyden chamber cell migration assay.** *A*, photographs of cells migrated through the filter. 1.5×10^6 cells in DMEM containing 10% FBS after detachment were added to the upper well of the chamber with the lower well filled with DMEM containing 10% FBS. Cells were allowed to migrate through polyvinylpyrrolidine-free filters with a pore size of 8 μm (Neuroprobe) coated with fibronectin (10 μg/ml) (Sigma) for 4 h. Cells that had migrated through the filter were fixed by methanol, exposed to Giemsa staining, and visualized by a microscope at a magnification of 200×. *B*, quantitative analysis of the number of cells on the filter. The number of cells migrated through and spread on the filter was counted from at least eight fields (*error bars* show the standard deviation). Results presented here are representative mean values of four experiments with three independent clones from each cell line.

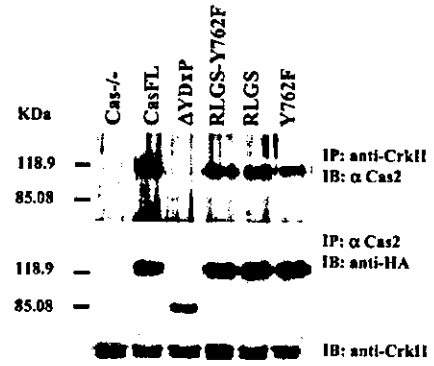

FIG. 5. **Association of Cas mutants with CrkII.** Cells plated on plastic culture dishes for 48 h were lysed using 1% Triton X-100 buffer as described under "Experimental Procedures." Equal portions of cell lysates were immunoprecipitated by antibody against CrkII (Santa Cruz Biotechnology), and immunoprecipitates were subjected to immunoblot by αCas2 antibody. As a control, an amount equal to the total amount of cell lysates was immunoprecipitated by antibody HA and then immunoblotted using αCas2 antibody. The expression of CrkII was indicated by Western blotting of the same quantity of whole cell lysates.

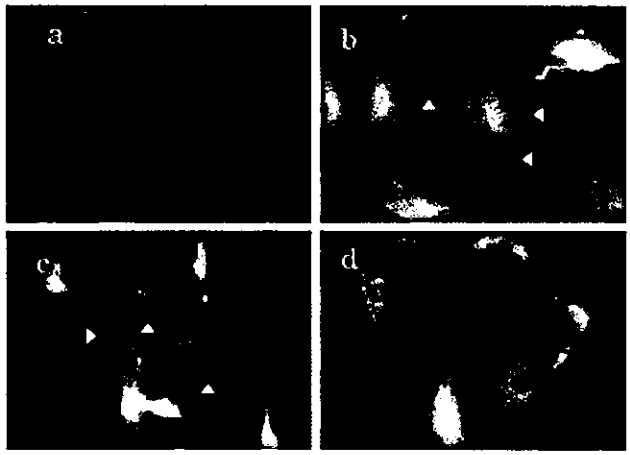

FIG. 6. **Localization of Cas mutants.** Localization of CasFL, ΔYDxP, and RLGS-Y762F stably expressed in Cas−/− fibroblasts was investigated by immunofluorescence using αCas2 antibody against Cas. Cells allowed to grow in a chamber slide for 48 h in DMEM with 10% FBS were fixed and stained by primary antibody αCas2 (10 ng/μl) and secondary antibody FITC-conjugated anti-rabbit (1:40) (Santa Cruz Biotechnology). Cells were then visualized by an Olympus fluorescence microscope with a 200× objective. *a*, Cas−/−; *b*, CasFL; *c*, ΔYDxP; *d*, RLGS-Y762F. The *arrowheads* show membrane-located fractions of CasFL and ΔYDxP mutants.

underlying the observations described above, phosphorylation of Cas mutants in Cas−/− and Cas−/−Src fibroblasts was investigated. Phosphorylation of ΔYDxP was at a level similar to CasFL in Cas −/− fibroblasts, whereas phosphorylation level of ΔSB and ΔSH3·SB was much lower (Fig. 8*A*). In Cas−/−Src cell lines, tyrosine phosphorylation of ΔSB, RLGS, and RLGS-Y762F mutants was significantly reduced compared with ΔSH3, ΔYDxP, ΔSH3·YDxP, and CasFL (Fig. 8*B*). It was revealed that the SB domain is essential for phosphorylation of Cas expressed in Cas−/− fibroblasts both in the absence and presence of activated Src. Finally, the results from all of the compensation assays done in this study demonstrated distinct roles for the individual signaling domains of Cas in the biological processes of fibroblasts (summarized in Table I).

DISCUSSION

This study revealed the domain functions of Cas through an investigation of the ability of a series of systemic mutants of Cas to rescue actin stress fiber organization, cell migration, and Src transformation that were impaired in Cas-deficient fibroblasts. As a result, the YDxP motifs were shown to be indispensable for actin stress fiber organization and to play essential roles in cell migration. Moreover, it was demonstrated that the SB domain was another critical region of dynamic regulation of cell motility, possibly because it plays an essential role in the membrane localization of Cas. Furthermore, it was shown that the SB domain was the vital region for anchorage-independent growth caused by activated Src, presumably because this region promotes tyrosine phosphorylation of Cas by direct association with activated Src.

YDxP Motifs in the SD Domain Are Indispensable for Actin Stress Fiber Organization and Cell Migration—No detectable difference in tyrosine phosphorylation and subcellular localization between the ΔYDxP mutant and CasFL was identified in Cas−/− fibroblasts. This fact suggests that phosphorylation at YDxP motifs is a minor portion of the whole tyrosine phosphorylation of Cas and is not critical for anchoring sites to the cellular membrane. The basal level of phosphorylation of YDxP

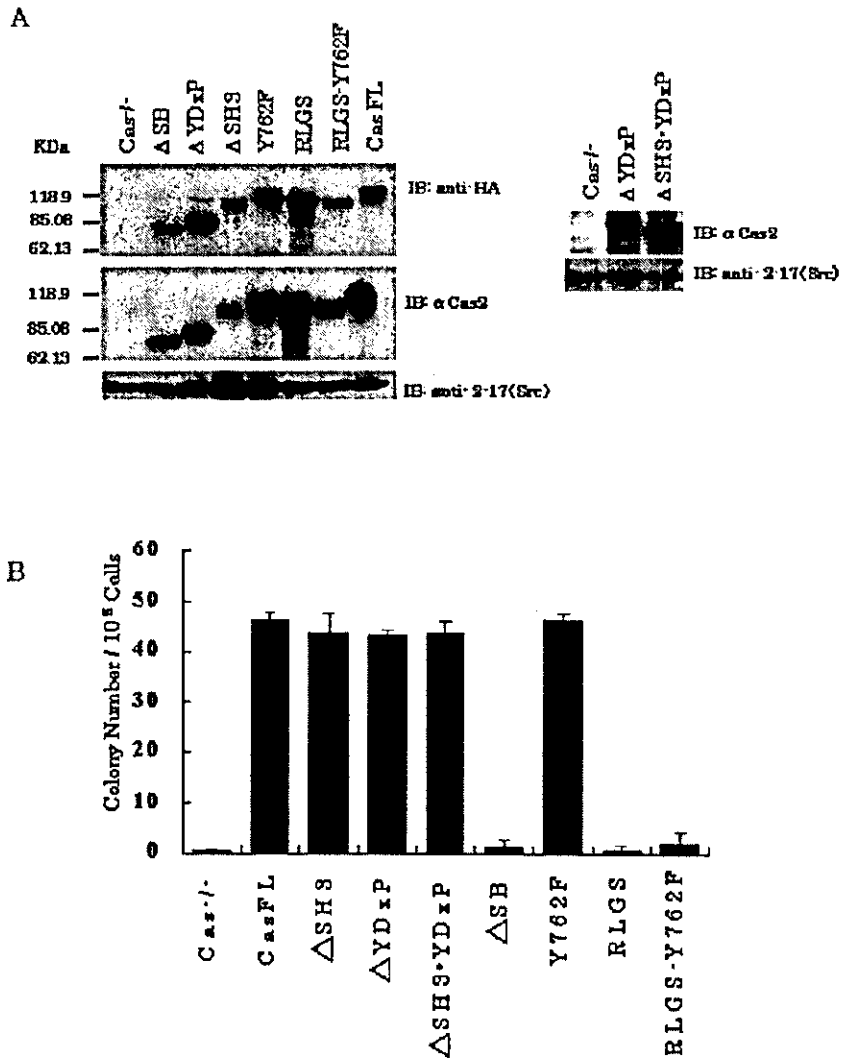

FIG. 7. **Establishment of cell lines stably expressing various Cas mutants in Cas−/− Src fibroblasts and soft agar colony formation assay results.** *A*, establishment of cell lines stably expressing CasFL, mutants of ΔSB, ΔYDxP, ΔSH3, Y762F, RLGS, RLGS-Y762F (*left panel*), or ΔSH3-YDxP (*right panel*) in Cas−/−Src fibroblasts. Expression of Cas mutants and full-length Cas were confirmed using αCas2 and anti-HA antibody. Expression of 527F-c-Src was confirmed by monoclonal anti-Src antibody 2-17. *B*, results of a soft agar colony formation assay. 10^5 cells resuspended in DMEM containing 10% FBS and 4% SeaPlaque GTG agarose were poured onto bottom agar containing 10% FBS and 0.53% agarose in 6-cm culture dishes (*error bars* show the standard deviation). Colonies containing more than 5 cells were counted under a microscope 14 days later. Results shown here are the average values of four replicated experiments.

motifs might be enough for the induction of actin stress fibers organization. A processive phosphorylation mechanism has been presented, to predict a type of autonomous function of YDxP motifs by using repetitive YDxP sequences as targets of both tyrosine kinases and SH2 domains (3, 26); this could explain an action of YDxP motifs independently of other domains of Cas. The influence of YDxP motifs on actin stress fiber organization is exerted by physical connections with specific molecules in phosphorylation-dependent manners. Previous studies have shown that CrkII and Nck are associated with Cas in actin cytoskeleton organization and cell migration (4, 27). The CrkII SH2 domain has a binding preference for YDxP motifs found in the substrate domain of Cas (25). In our study, ΔYDxP actually lacks the association with CrkII, which may be responsible for the defect in actin stress fiber formation. No detectable association of adaptor protein Nck with any mutant was identified in Cas−/− fibroblasts (data not shown). The CrkII-C3G pathway, which is reported to activate the Rho family of small GTP-binding proteins, is closely involved in the process of actin organization and cell migration (27, 28). However, there remains the possibility that other SH2-containing molecules binding to YDxP motifs of Cas regulate actin biosynthesis.

LPA, a strong activator of Rho family GTPases, has been reported to induce phosphorylation of Cas (12). The fact that it could stimulate the formation of actin stress fibers in the absence of Cas indicates that direct target proteins of LPA are not located upstream of Cas in the signaling pathway but are found either downstream or in different pathways in actin stress fiber organization.

The RPLP Motif in the SB Domain Is Another Motif Essential for Cell Migration—The finding that ΔYDxP also showed a significant defect in cell migration could be explained by previous study showing that actin stress fiber formation is one of the critical step in cell migration (29). It was also known from analysis of the ΔSB mutant that cell migration additionally requires the Src-binding domain of Cas, which, by binding Src-family kinases, promote tyrosine phosphorylation and the subsequent membrane localization of Cas. Previous reports also suggest these functions of the Src-binding domain in normal fibroblasts (2, 16, 30). In this case, Fyn and Src kinases have been identified as Src-family kinases responsible for phosphorylation of Cas in fibroblasts (13, 15). A high level of tyrosine phosphorylation, which may involve phosphorylation at specific tyrosine residues of Cas protein, will be required for association with special sets of signaling molecules and for the completion of cell migration. A similar case was found in Src/Yes/Fyn (SYF)-deficient fibroblasts, which showed a decreased level of adhesion-dependent Cas phosphorylation and exhibited marked defects in cell migration (31). The interaction between

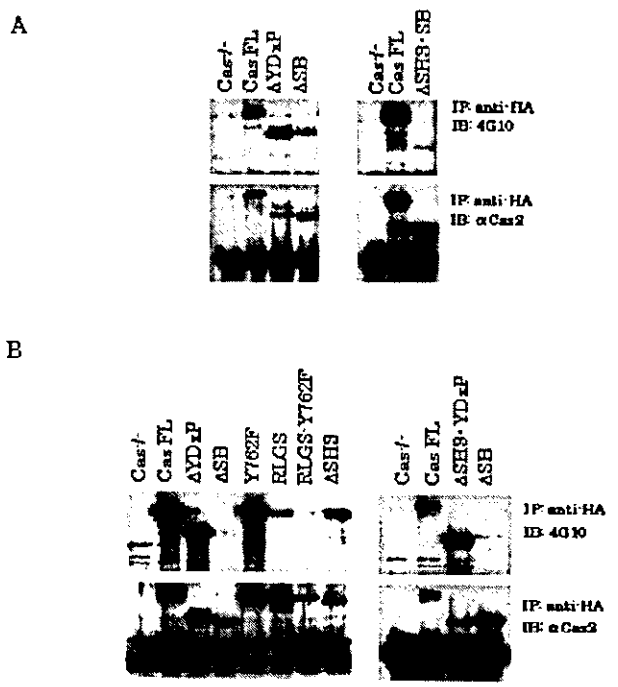

FIG. 8. **Phosphorylation of Cas mutants stably expressed in Cas−/− or Cas−/−Src fibroblasts.** Phosphotyrosine of Cas mutants re-expressed in Cas−/− or Cas−/−Src fibroblasts were determined by immunoblotting an equal portions of the immunoprecipitates with anti-phosphotyrosine antibody 4G10 (Upstate Biotechnology). The same membrane was reblotted using anti-HA antibody to indicate the quantity of immunoprecipitates. *A*, low phosphorylation level of ΔSB (*left panel*) and ΔSH3·SB (*right panel*) in Cas−/− fibroblasts. *B*, phosphorylation of Cas mutants in Cas−/−Src fibroblasts (*left panel*) and decreased phosphorylation of ΔSB compared with that of ΔSH3·YDxP in Cas−/−Src fibroblasts (*right panel*).

TABLE I

Summary of the rescue ability of Cas mutants in actin stress fiber organization, cell migration, and Src transformation

N, not tested; −, no compensation; +, compensation; ++, excessive compensation.

Cell lines	Actin stress fibers	Cell migration	Soft agar colonies
Cas−/−	−	−	−
CasFL	+	+	+
ΔSH3	++	+	+
ΔSD	−	−	N
ΔYQxP	+/−	−	N
ΔYDxP	−	−	+
ΔSB	++	−	−
Y762F	+	+	+
RLGS	+	−	−
RLGS-Y762F	++	−	−
ΔSH3·SB	++	−	N
ΔSH3·YDxP	N	N	+

Src and Cas occurs mainly between the SH3 domain of Src and the RPLPSPP motif of Cas, located within the SB domain (6). Consistent with this observation, cell mobility was almost completely restored by Y762F but very poorly by RLGS in Cas−/− fibroblasts. These results indicate that the RPLP motif that sustains Src-Cas association plays an essential role in cell migration.

The ΔSH3 mutant could rescue both the organization of actin stress fibers and cell migration of Cas−/− fibroblasts, although it was suggested that the SH3 domain of Cas was involved in cell migration through direct binding with FAK and PTP-PEST (17, 19). There is another model showing that Src serve as a bridge between FAK and Cas by its SH2 and SH3 domains (4). There is also a report that integrin-mediated phosphorylation of Cas is not compromised in fibroblasts lacking FAK but significantly reduced in cells lacking Src (14). In light of these studies, there might be alternative pathways utilizing the SB domain of Cas via FAK and Src family kinases in actin stress fiber organization and cell migration. Cas is a specific substrate of the protein tyrosine phosphatase PTP-PEST (32). From our results, it was suggested that either action of PTP-PEST does not require association at the SH3 domain of Cas or that PTP-PEST itself is dispensable for some biological activities of Cas. We failed to establish Cas−/− fibroblast lines expressing comparable level of ΔYQxP to other mutants, although we tried several independent transfections. No rescue of cell motility by ΔYQxP was observed, perhaps because of its lower expression level. However, it was observed that ΔYQxP could rescue the organization of actin stress fibers, indicating that YQxP motifs are dispensable for this process.

The SB Domain Is Indispensable for Src Transformation—It was revealed that the SB domain of Cas also plays indispensable roles in anchorage-independent growth by activated Src. The reduced phosphorylation level of Cas caused by deletion of the SB domain was observed also in Cas−/− Src fibroblasts. Similar to the case of Cas and normal Src family kinases in Cas−/− fibroblasts, the association between Cas and activated Src kinase is essential for tyrosine phosphorylation of Cas by activated Src, which results in cellular transformation. Consistent with our results, a previous study revealed that C-terminal Src-binding sequence of Cas can functionally substitute for full-length endogenous Cas in transformation of rat 1-LA29 cells (33). Interestingly, YDxP sequences that are critical for actin stress fiber formation are not required for cell transformation in either case. Hyperphosphorylation at tyrosines around Src-binding domain of Cas caused by the activated Src might be critical for the signaling of cellular transformation. In fact, hyperphosphorylation of Cas was frequently found in malignant solid tumor cell lines such as melanoma, colon cancer, seminoma, and glioblastoma (data not shown) although the meaning of tyrosine phosphorylation of Cas in cancer cells is not clear so far. It will require further investigation to identify the specific tyrosine phosphorylation sites in Cas that play critical roles in anchorage-independent growth in cell transformation.

In conclusion, this study has given insight into the domain functions of Cas using a compensation assay of Cas−/− fibroblasts. Cas keeps the signal equilibrium of actin cytoskeleton organization, cell migration, and Src transformation by utilizing different domains in differential and cooperative ways. In addition, important roles of direct Cas-Src association and phosphorylation of Cas in cell migration and transformation were observed. Further research is required for the clarification of downstream effectors regulated by functional motifs or domains identified in each process above.

REFERENCES

1. Reynolds, A. B., Kanner, S. B., Wang, H. C., and Parsons, J. T. (1989) *Mol. Cell. Biol.* **9**, 3951–3958
2. Sakai, R., Iwamatsu, A., Hirano, N., Ogawa, S., Tanaka, T., Mano, H., Yazaki, Y., and Hirai, H. (1994) *EMBO J.* **13**, 3748–3756
3. Mayer, B. J., Hirai, H., and Sakai, R. (1995) *Curr. Biol.* **5**, 296–305
4. Schlaepfer, D. D., Broome, M. A., and Hunter, T. (1997) *Mol. Cell. Biol.* **17**, 1702–1713
5. Prasad, N., Topping, R. S., and Decker, S. J. (2001) *Mol. Cell. Biol.* **21**, 1416–1428
6. Nakamoto, T., Sakai, R., Ozawa, K., Yazaki, Y., and Hirai, H. (1996) *J. Biol. Chem.* **271**, 8959–8965
7. Polte, T. R., and Hanks, S. K. (1995) *Proc. Natl. Acad. Sci. U. S. A.* **92**, 10678–10682
8. Kirsch, K. H., Georgescu, M. M., and Hanafusa, H. (1998) *J. Biol. Chem.* **273**, 25673–25679
9. Garton, A. J., Burnham, M. R., Bouton, A. H., and Tonks, N. K. (1997) *Oncogene* **15**, 877–885
10. Nojima, Y., Morino, N., Mimura, T., Hamasaki, K., Furuya, H., Sakai, R., Sato,

T., Tachibana, K., Morimoto, C., Yazaki, Y., and Hirai, H. (1995) *J. Biol. Chem.* **270,** 15398–15402
11. Vuori, K., and Ruoslahti, E. (1995) *J. Biol. Chem.* **270,** 22259–22262
12. Casamassima, A., and Rozengurt, E. (1997) *J. Biol. Chem.* **272,** 9363–9370
13. Hamasaki, K., Mimura, T., Morino, N., Furuya, H., Nakamoto, T., Aizawa, S., Morimoto, C., Yazaki, Y., Hirai, H., and Nojima, Y. (1996) *Biochem. Biophys. Res. Commun.* **222,** 338–343
14. Vuori, K., Hirai, H., Aizawa, S., and Ruoslahti, E. (1996) *Mol. Cell. Biol.* **16,** 2606–2613
15. Sakai, R., Nakamoto, T., Ozawa, K., Aizawa, S., and Hirai, H. (1997) *Oncogene* **14,** 1419–1426
16. Burnham, M. R., Bruce-Staskal, P. J., Harte, M. T., Weidow, C. L., Ma, A., Weed, S. A., and Bouton, A. H. (2000) *Mol. Cell. Biol.* **20,** 5865–5878
17. Cary, L. A., Han, D. C., Polte, T. R., Hanks, S. K., and Guan, J. L. (1998) *J. Cell Biol.* **140,** 211–221
18. Klemke, R. L., Leng, J., Molander, R., Brooks, P. C., Vuori, K., and Cheresh, D. A. (1998) *J. Cell Biol.* **140,** 961–972
19. Garton, A. J., and Tonks, N. K. (1999) *J. Biol. Chem.* **274,** 3811–3818
20. Auvinen, M., Paasinen-Sohns, A., Hirai, H., Andersson, L. C., and Holtta, E. (1995) *Mol. Cell. Biol.* **15,** 6513–6525
21. Honda, H., Oda, H., Nakamoto, T., Honda, Z., Sakai, R., Suzuki, T., Saito, T., Nakamura, K., Nakao, K., Ishikawa, T., Katsuki, M., Yazaki, Y., and Hirai, H. (1998) *Nat. Genet.* **19,** 361–365
22. Honda, H., Nakamoto, T., Sakai, R., and Hirai, H. (1999) *Biochem. Biophys. Res. Commun.* **262,** 25–30
23. Nakamoto, T., Sakai, R., Honda, H., Ogawa, S., Ueno, H., Suzuki, T., Aizawa, S., Yazaki, Y., and Hirai, H. (1997) *Mol. Cell. Biol.* **17,** 3884–3897
24. Schmitz, A. A., Govek, E. E., Bottner, B., and Van Aelst, L. (2000) *Exp. Cell Res.* **261,** 1–12
25. Songyang, Z., Shoelson, S. E., Chaudhuri, M., Gish, G., Pawson, T., Haser, W. G., King, F., Roberts, T., Ratnofsky, S., Lechleider, R. J., Neel, B. G., Birge, R. B., Eduardo Fajardo, J., Chou, M. M., Hanafusa, H., Schaffhausen, B., and Cantley, L. C. (1993) *Cell* **72,** 767–778
26. Pawson, T. (1995) *Nature* **373,** 477–478
27. Kiyokawa, E., Hashimoto, Y., Kobayashi, S., Sugimura, H., Kurata, T., and Matsuda, M. (1998) *Genes Dev.* **12,** 3331–3336
28. Kiyokawa, E., Hashimoto, Y., Kurata, T., Sugimura, H., and Matsuda, M. (1998) *J. Biol. Chem.* **273,** 24479–24484
29. Mitchison, T. J., and Cramer, L. P. (1996) *Cell* **84,** 371–379
30. Pellicena, P., and Miller, W. T. (2001) *J. Biol. Chem.* **276,** 28190–28196
31. Klinghoffer, R. A., Sachsenmaier, C., Cooper, J. A., and Soriano, P. (1999) *EMBO J.* **18,** 2459–2471
32. Garton, A. J., Flint, A. J., and Tonks, N. K. (1996) *Mol. Cell. Biol.* **16,** 6408–6418
33. Burnham, M. R., Harte, M. T., and Bouton, A. H. (1999) *Mol. Carcinog.* **26,** 20–31

THE JOURNAL OF BIOLOGICAL CHEMISTRY
Vol. 278, No. 48, Issue of November 28, pp. 48367–48376, 2003
Printed in U.S.A.

Cooperative Roles of Fyn and Cortactin in Cell Migration of Metastatic Murine Melanoma*

Received for publication, July 28, 2003, and in revised form, September 12, 2003
Published, JBC Papers in Press, September 16, 2003, DOI 10.1074/jbc.M308213200

Jinhong Huang‡§¶, Tamae Asawa‡, Tsuyoshi Takato‖, and Ryuichi Sakai‡**

From the ‡Growth Factor Division, National Cancer Center Research Institute, 5-1-1 Tsukiji, Chuo-ku, Tokyo 104-0045, Japan, the ‖Department of Oral and Maxillofacial Surgery, University of Tokyo, 7-3-1 Hongo, Bunkyo-ku, Tokyo 113-8655, Japan, and the §Laboratory for Molecular Neurogenesis, RIKEN Brain Science Institute, 2-1 Hirosawa, Wako, Saitama 351-0198, Japan

Src family kinases are major regulators of various integrin-mediated biological processes, although their functional roles and substrates in cancer metastasis are unknown. We explored the roles of Src family tyrosine kinases in cell migration and the spread of K-1735 murine melanoma cell lines with low or high metastatic potential. Corresponding to elevated cell motility and spreading ability, Fyn was selectively activated among Src family kinases, and the cell motility was blocked by an inhibitor of Src family kinases. Significant tyrosine phosphorylation of cortactin, stable complex formation between activated Fyn and cortactin, and co-localization of cortactin with Fyn at cell membranes were all observed only in cells with high metastatic potential. Both integrin-mediated Fyn activation and hyperphosphorylation of cortactin were observed 2–5 h after stimulation in highly metastatic cells, and they required *de novo* protein synthesis. We demonstrate that cortactin is a specific substrate and cooperative effector of Fyn in integrin-mediated signaling processes regulating metastatic potential.

Malignant tumors are thought to contain subpopulations of cells with differential metastatic capabilities (1). Processes of tumor metastasis consist of multiple steps linked together, including invasion, detachment, intravasation, circulation, adhesion, extravasation, and growth in distant organs (2). Cell locomotion and spreading are key functions of the cells required in most of these processes. Analysis of differences in expression and modification of signaling molecules associated with cell migration and spreading among tumor sublines with different metastatic potentials in a tumor is expected to provide precise information for understanding the molecular mechanisms underlying the development of cancer metastasis.

There are studies demonstrating that Src family tyrosine kinases play essential roles in the signaling of integrin-mediated biological processes such as actin organization and cell migration (3–7). In addition, recent reports show that Src is highly activated in colon cancers, particularly in those metastatic to the liver (8). Involvement of Src kinase during metastatic spread of carcinoma cells in NBT-II rat carcinoma cell lines has also been suggested (5). Fyn has been suggested a factor governing the metastatic potential of tumors including murine methylcholanthrene-induced fibrosarcoma cells (9), although the precise mechanism is unknown.

Increasing numbers of studies have shown that Src family kinases function through collaboration with their substrates, such as FAK, cortactin, $p130^{Cas}$ (a Crk-associated substrate), and paxillin in cytoskeleton organization and cell migration. FAK is activated upon cell binding to extracellular matrix proteins and forms transient signaling complexes with Src family kinases (10). Cortactin plays essential roles in cortical actin cytoskeleton organization, primarily affecting cell motility and invasion (11–13). A docking protein, $p130^{Cas}$, plays essential roles in cell attachment and migration when it is tyrosine-phosphorylated by Src family kinases (6). Functional roles of paxillin in integrin-mediated signaling have been implicated by tyrosine phosphorylation of paxillin following integrin-dependent cell adhesion to extracellular matrix proteins, which is in part attributed to Src family kinases (14). To obtain further information on their involvements in the progression of metastasis, appropriate biological models showing different metastatic potentials are required.

A widely used model for studying the molecular mechanisms underlying the progression of metastasis is a series of cell lines derived from K-1735 murine melanoma, which contains heterogeneous clones with multiple metastatic diversities (15). The primary K-1735 melanoma that arose in an inbred C3H/HeN murine mammary tumor virus-negative mouse was transplanted once into an immunosuppressed recipient and then established in culture. Randomly chosen clones C10 and C19 were classified as nonmetastatic or low metastatic; M2 and X21 were highly metastatic and produce tumor foci in lungs of syngenic mice (15). In this study, we investigated the roles of Src family tyrosine kinases in cell migration and the spread of these cell lines. Up-regulation of Fyn kinase activity and enhanced tyrosine phosphorylation of cortactin were identified in highly metastatic cells, which also showed elevated cell motility and spreading ability. A new mode of integrin-mediated activation of Fyn was also observed in highly metastatic cells. These results indicate a novel role of the Fyn-cortactin pathway required for the regulation of cell motility and metastatic potential during the progression of metastasis.

EXPERIMENTAL PROCEDURES

Cells and Cell Culture—K-1735-derived mouse melanoma cell lines were donated by Dr. I. J. Fidler. Clones C-10 and C-19 are classified as nonmetastatic or low metastatic. Parental clones M-2 and X21 are highly metastatic and produce tumor foci in lungs of syngenic mice (15).

* This work was supported by the Program for Promotion of Fundamental Studies in Health Science of Organization for Pharmaceutical Safety and Research of Japan. The costs of publication of this article were defrayed in part by the payment of page charges. This article must therefore be hereby marked "*advertisement*" in accordance with 18 U.S.C. Section 1734 solely to indicate this fact.

¶ Supported by a scholarship from HonJo International Scholarship Foundation.

** To whom correspondence should be addressed: Growth Factor Division, National Cancer Center Research Institute, 5-1-1 Tsukiji, Chuo-ku, Tokyo 104-0045, Japan. Tel: 03-3542-2511 (ext. 4300); Fax: 03-3542-8170; E-mail: rsakai@gan2.res.ncc.go.jp.

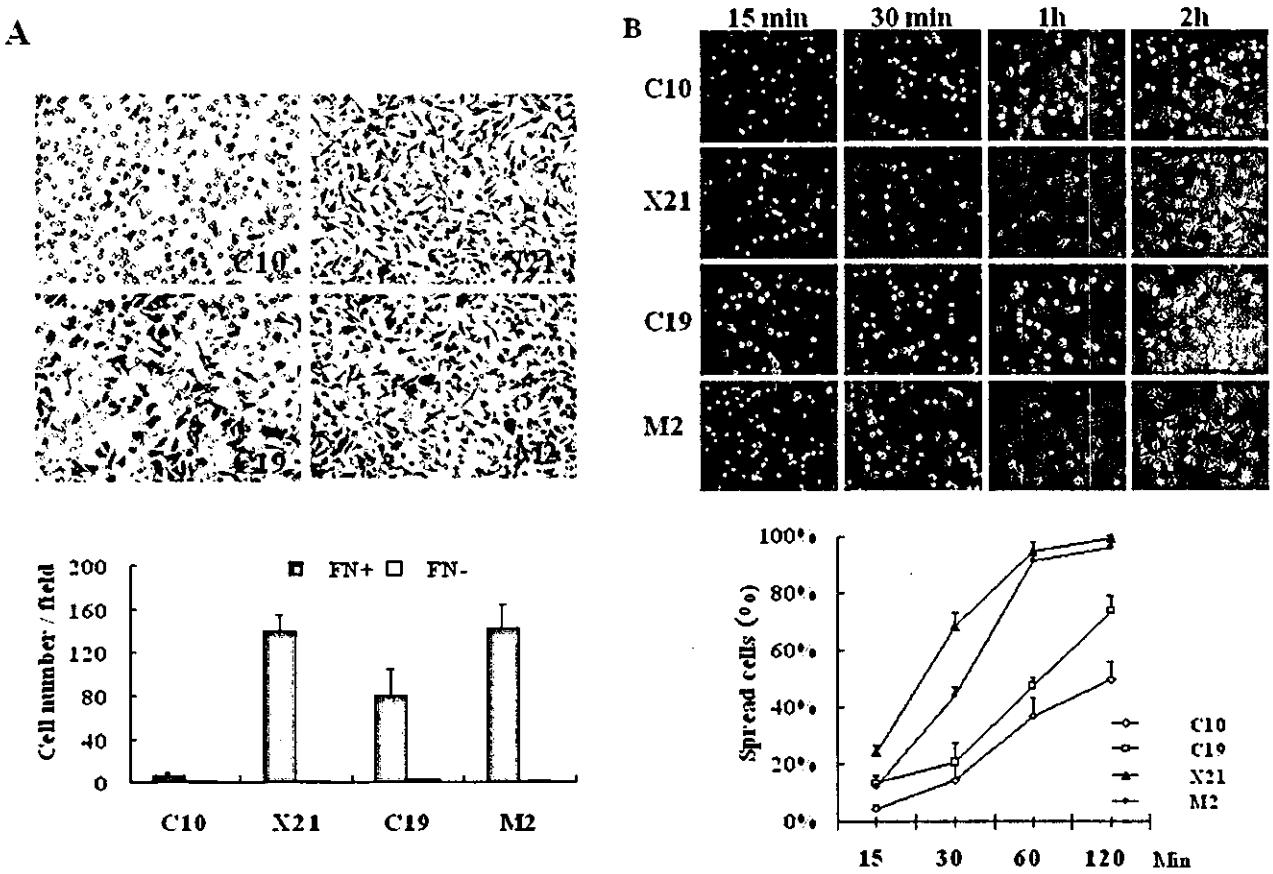

FIG. 1. **Enhanced motility and spreading ability on FN in highly metastatic murine melanoma cell lines.** *A*, cell motility under FN stimulation was elevated in highly metastatic cells. Haptotactic cell migration toward FN was measured using modified Boyden chamber cell migration assay as described under "Experimental Procedures." Cells migrated through the filter in 3 h and spread on the lower side of the filter were fixed, exposed to Giemsa staining, and visualized by a microscope at a magnification of 200×. The number of cells was counted from at least eight microscope fields. The *error bars* show the standard deviation. *B*, enhanced cell spreading ability of highly metastatic cells. A cell spreading assay was carried out as described under "Experimental Procedures." 10^5/ml cells in DMEM containing 0.5% FCS were plated on FN-coated dishes (10 μg/ml). Photos of cells were taken under the microscope at a magnification of 200× at the indicated times. Single cells that were phase bright with rounded morphology were scored as nonspread, whereas those that possessed a flat shape and were phase dark were scored as spread. The percentages of spread cells at each time point were scored as indicated. The same experiment was repeated at least three times, and the *error bars* show the standard deviation.

3Y1-Crk is an isolated clone of rat 3Y1 cells transfected with v-Crk cDNA of an avian sarcoma virus CT10 inserted in expression vector pMV-7. 3Y1-Vec is an isolated clone of rat 3Y1 cells transfected with expression vector pMV-7 (16). All tumor cells were maintained in Dulbecco's modified Eagle's medium (DMEM[1]; Sigma) supplemented with 10% fetal calf serum (FCS; Sigma) and grown in the presence of penicillin and streptomycin (Sigma) at 37 °C with 5% CO_2.

Antibodies and Reagents—Polyclonal antibodies against Src family tyrosine kinase (Src-2), Src (Src-N-16), or Fyn (Fyn3) were obtained from Santa Cruz Biotechnology. Anti-phosphotyrosine antibody 4G10, polyclonal antibody against human Fyn, and monoclonal antibody against cortactin (clone 4F11) were obtained from Upstate Biotechnology, Inc. Monoclonal antibodies against Yes, Hck, or FAK were obtained from Transductory Laboratories. Monoclonal antibody against paxillin was obtained from Zymed Laboratories Inc. Polyclonal antibodies against Cas (Cas3 and Cas2) were used as described previously (16). Rhodamine-labeled phalloidin was purchased from Molecular Probes, and fluorescein isothiocyanate-conjugated anti-mouse and rhodamine-conjugated anti-rabbit antibodies were obtained from Santa Cruz Biotechnology. Polylysine, fibronectin, and cycloheximide were purchased from Sigma. Src family kinases inhibitor 4-amino-5-(4-chlorophenyl)-7-(t-butyl)pyrazolo[3,4-d]pyrimidine (PP2) and the structural analog 4-amino-7-phenylpyrazol [3,4-d]pyrimidine (PP3) were obtained from Calbiochem-Novabiochem Ltd.

Cell Stimulation with Fibronectin or Polylysine—The cells were serum-starved (on dish) in DMEM containing 0.5% FCS for 18 h, washed by phosphate-buffered saline (PBS), and harvested by trypsin-EDTA treatment (0.5% trypsin, 2 mM EDTA) in DMEM. The trypsin was inactivated by the addition of soybean trypsin inhibitor (0.5 mg/ml) (Sigma), and the cells were collected by centrifugation, resuspended in DMEM containing 0.5% FCS, and held in suspension for 30 min at 37 °C (off dish). The cell culture dishes were precoated with FN purified from bovine plasma (10 μg/ml) or polylysine (10 μg/ml) (Sigma) in PBS overnight at 4 °C, rinsed with PBS, and warmed to 37 °C for 1 h. Suspended cells were distributed onto ligand-coated dishes and incubated at 37 °C. At various times following plating as indicated, the attached cells were rinsed in PBS and lysed in 1% Triton X-100 buffer (see below). Total cell proteins in lysates were standardized prior to use.

Cell Lysis, Immunoblotting, and Immunoprecipitation—Protein extraction and Western blotting analysis were performed as described (6). Briefly, the cells were lysed in 1% Triton X-100 buffer (50 mM Hepes, 150 mM NaCl, 10% glycerol, 1% Triton X-100, 1.5 mM $MgCl_2$, 1 mM EGTA, 100 mM NaF, 1 mM Na_3VO_4, 10 μg/ml approtinin, 10 μg/ml leupeptin, 1 mM phenylmethylsulfonyl), and insoluble material was removed by centrifugation. The protein aliquots were separated by SDS-PAGE and probed with 1:2000 diluted antibodies. For immunoprecipitation, 500 μg of protein was mixed with 1–2 μg of antibodies against cortactin, Src family (Src-2), Src (Src-N-16), Fyn, Cas3, paxillin, or FAK and incubated for 1 h on ice. Then samples were rotated with

[1] The abbreviations used are: DMEM, Dulbecco's modified Eagle's medium; FCS, fetal calf serum; PP2, 4-amino-5-(4-chlorophenyl)-7-(t-butyl)pyrazolo[3,4-d]pyrimidine; PP3, 4-amino-7-phenylpyrazol [3,4-d]pyrimidine; FN, fibronectin; PBS, phosphate-buffered saline; CHX, cycloheximide.

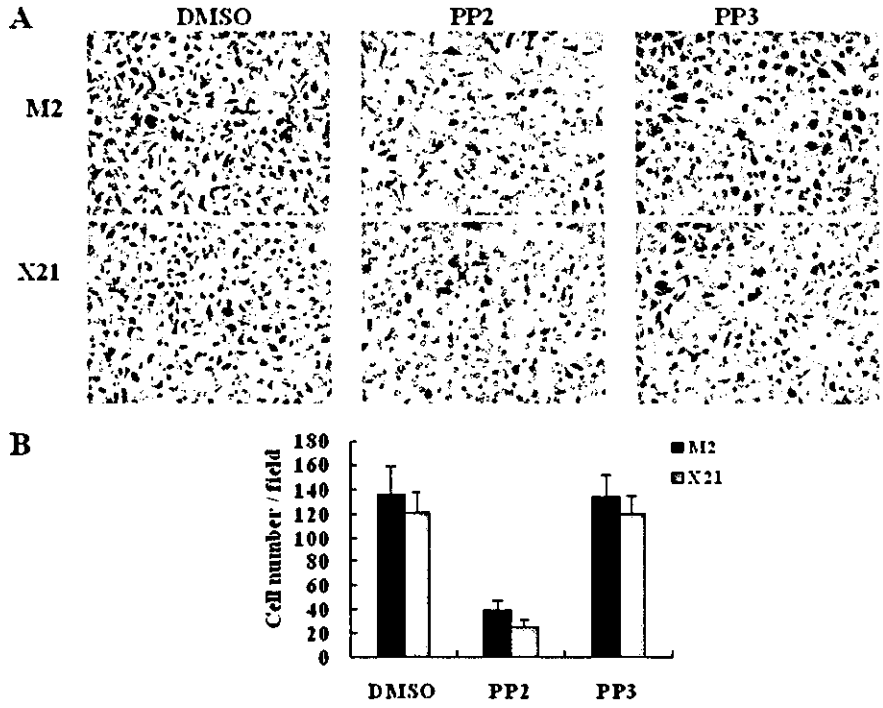

FIG. 2. **Impaired cell motility by PP2 treatment in highly metastatic murine melanoma cells.** The cells were subjected to haptotactic cell migration toward FN using a Boyden chamber in the presence of PP2 (10 μM), dimethyl sulfoxide (*DMSO*, 10 μM), or PP3 (10 μM) in the upper well as described under "Experimental Procedures." The cells were allowed to move in 3 h toward FN added to the lower chamber; the cells at the lower side of the filter were exposed to Giemsa staining and visualized under microscope at a magnification of 200×. The number of cells on the lower side of the filter was counted from at least eight fields (*error bars* show the standard deviation). The results presented here are representative mean values of experiments performed four times.

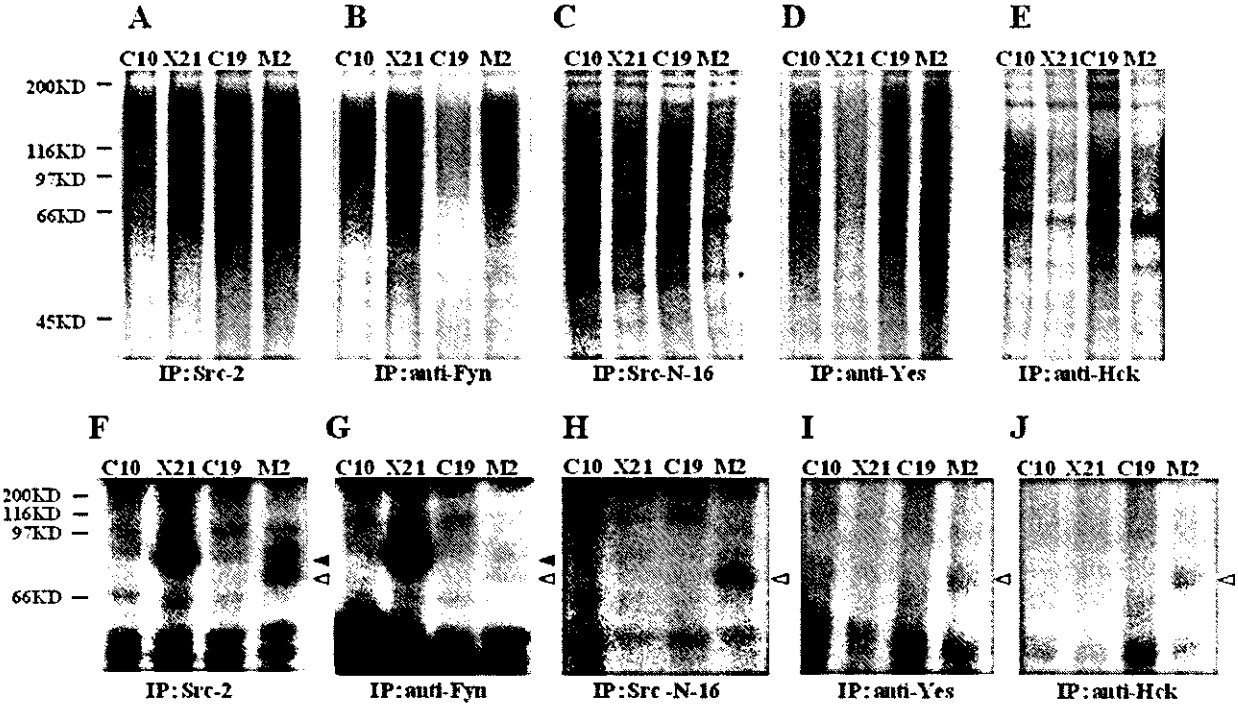

FIG. 3. **Elevated Fyn kinase activity and highly phosphorylated proteins associated with Fyn in cells with high metastatic potential.** The cells plated on plastic culture dishes for 48 h were lysed using 1% Triton X-100 buffer as described under "Experimental Procedures." Src family kinases in equal portions of cell lysates were isolated by immunoprecipitation (*IP*) using antibodies against Src family (Src2; *A* and *F*), Fyn (*B* and *G*), Src (Src-N-16; *C* and *H*), Yes (*D* and *I*), or Hck (*E* and *J*). The immunoprecipitates were labeled by [γ-^{32}P]ATP in an *in vitro* kinase assay in the presence (*A–E*) or absence (*F–J*) of exogenous synthetic polypeptides poly[Glu-Tyr]. The labeled proteins were analyzed by SDS-PAGE and visualized by autoradiography. The results presented here are representatives of experiments performed at least twice. *A–E*, kinase activities of Src family kinases in the presence of poly[Glu-Tyr]. Elevated Fyn activity in X21 and M2 was observed. *F–J*, phosphorylated proteins associated with Src family kinases in mildly or highly metastatic cells in an *in vitro* kinase assay. Fyn-associated proteins with a size of 85 kDa were specially observed in X21 and M2 (as indicated by *closed triangles*). Phosphorylated proteins with a size of 80 kDa in M2 associated with Src, Yes, and Hck in M2 are indicated by *open triangles*.

protein A- or protein G-Sepharose beads (Sigma) for 1 h at 4 °C. The beads were washed four times with 1% Triton X-100 buffer and boiled in sample buffer (2% SDS, 0.1 M Tris-HCl, pH 6.8, 10% glycerol, 0.01% bromphenol blue, 0.1 M dithiothreitol) before being subjected to SDS-PAGE analysis.

Immunofluorescence—Immunofluorescence staining was performed

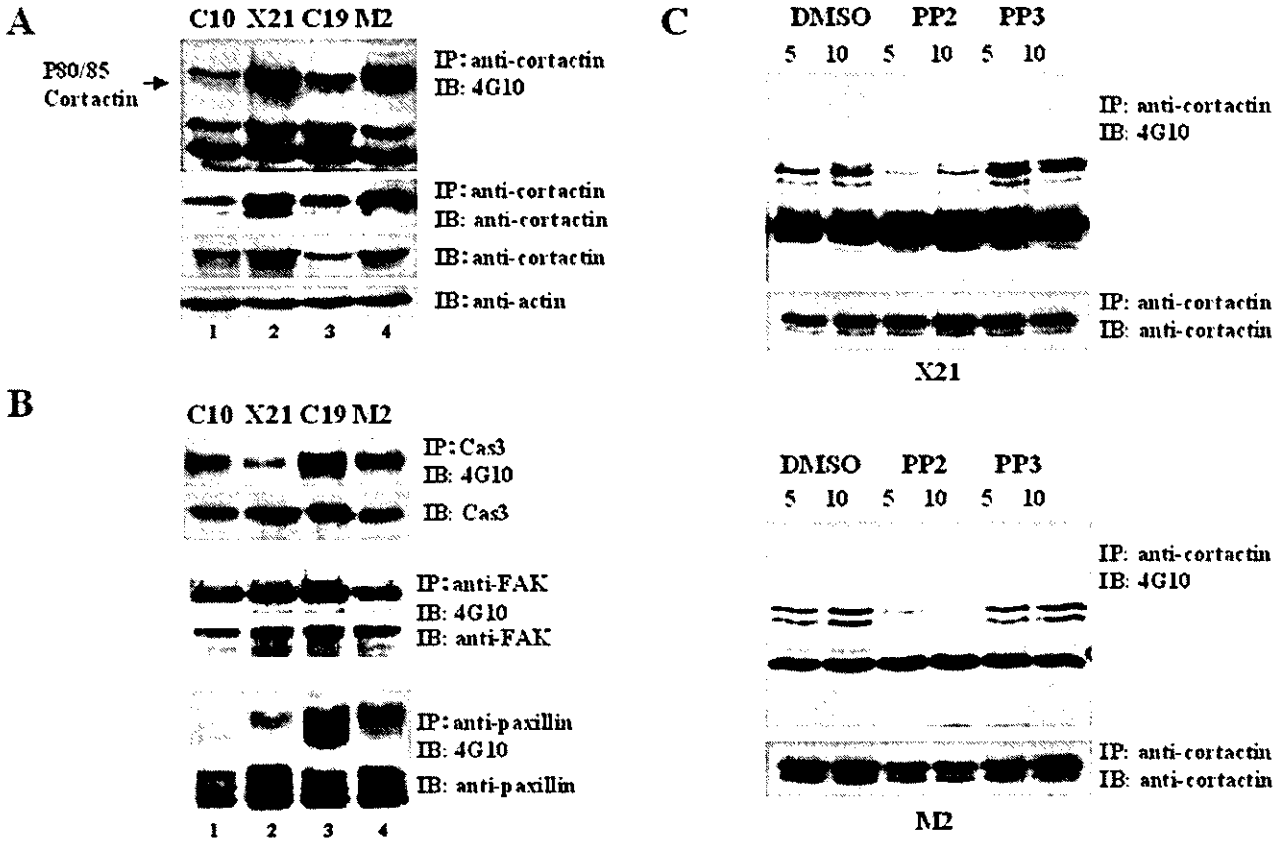

FIG. 4. **Overexpression and hyperphosphorylation of cortactin in cells with high metastatic potential.** Cells plated on plastic culture dishes for 48 h were lysed in 1% Triton X-100 buffer as described under "Experimental Procedures." Tyrosine phosphorylation of cortactin, $p130^{Cas}$, paxillin, and FAK in equal portions of cell lysates were analyzed by immunoprecipitation (*IP*) using antibody against cortactin (UBI), $p130^{Cas}$, paxillin (Zymed Laboratories Inc.), or FAK (Transduction Laboratories). The immunoprecipitates were subjected to immunoblotting analysis by anti-phosphotyrosine antibody 4G10. As a control, quantity of cortactin, $p130^{Cas}$, paxillin, or FAK in equal amount of whole cell lysates were also analyzed by immunoblotting (*IB*). *A*, expression and tyrosine phosphorylation of cortactin are up-regulated in highly metastatic cells X21 and M2. *B*, expression and tyrosine phosphorylation of $p130^{Cas}$, paxillin, and FAK in melanoma cells. *C*, PP2 treatment impaired tyrosine phosphorylation of cortactin in highly metastatic cell lines X21 (*upper panel*) and M2 (*lower panel*). The cells cultured in DMEM with 10% FCS were washed by DMEM and then treated by PP2 (10 μM), Me_2SO (10 μM), or PP3 (10 μM) in DMEM for 15 min before being lysed in 1% Triton X-100 buffer. Cortactin in equal portions of cell lysates was isolated by immunoprecipitation and subjected to immunoblotting by anti-phosphotyrosine antibody 4G10.

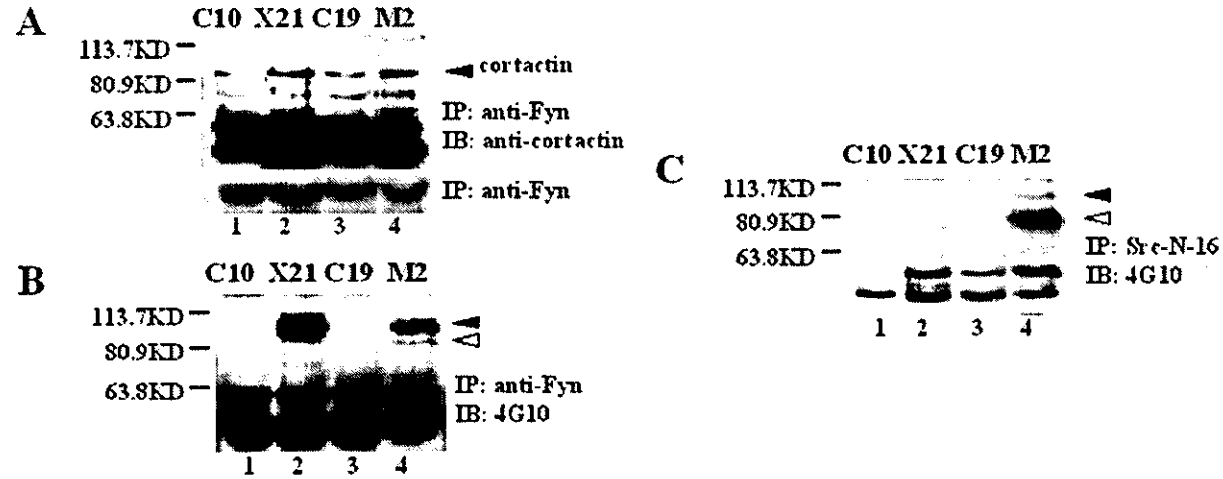

FIG. 5. **Specific association between cortactin and Fyn in highly metastatic melanoma cells.** *A*, physical association between cortactin and Fyn. Equal amounts of immunoprecipitates (*IP*) by antibody against Fyn (Fyn3) (Santa Cruz Biotechnology) were subjected to immunoblotting (*IB*) by anti-cortactin antibody. The expression of Fyn was indicated by immunoblotting analysis of equal amount of whole cell lysates using antibody against Fyn (Fyn3). Enhanced association between cortactin and Fyn in X21 and M2 were observed. *B* and *C*, tyrosine-phosphorylated proteins associated with Fyn (*B*) or Src (*C*) were analyzed by immunoblotting equal portion of immunoprecipitations against Fyn or Src (Src-N-16, Santa Cruz Biotechnology) with anti-phosphotyrosine antibody 4G10 (UBI). Tyrosine phosphorylation of Fyn-associated protein with a size of 85 kDa (indicated by *closed triangle*) in X21 and M2 and tyrosine phosphorylation of Src-associated protein in M2 with a size of 80 kDa (indicated by *open triangle*) were observed.

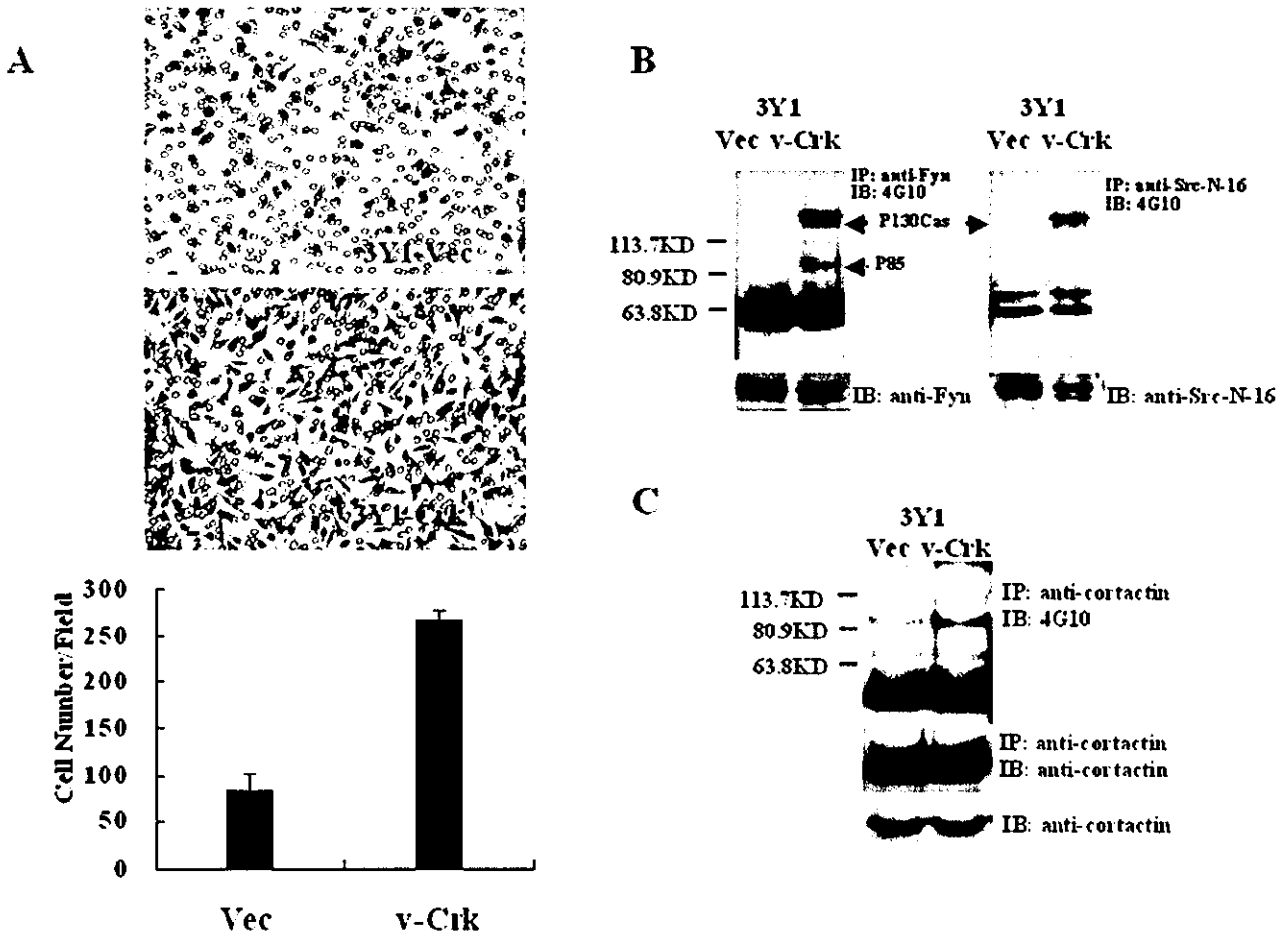

FIG. 6. **Fyn-cortactin association in 3Y1-Crk fibroblasts.** *A*, cell motility was enhanced in 3Y1-Crk fibroblasts. A modified Boyden chamber cell migration assay was performed as described under "Experimental Procedures." The cells that had migrated through the filter were fixed, exposed to Giemsa staining, and visualized by a microscope at a magnification of 200×. The number of cells on the lower side of the filter was counted from at least eight fields (*error bars* show the standard deviation). The results presented here are representative mean values of experiments performed three times. *B*, tyrosine-phosphorylated proteins $p130^{Cas}$ and P85 were associated with Fyn in 3Y1-Crk fibroblasts. *C*, elevated tyrosine phosphorylation of cortactin in 3Y1-Crk fibroblasts. Fyn-associated tyrosine-phosphorylated protein and phosphotyrosine of cortactin in 3Y1-Crk fibroblasts were determined by immunoblotting equal portion of immunoprecipitations (*IP*) against Fyn or cortactin (UBI) with anti-phosphotyrosine antibody 4G10 (UBI). The quantity of Fyn or cortactin in an equal amount of whole cell lysates was also analyzed by immunoblotting (*IB*).

essentially as described previously (6). 6×10^4 cells were plated onto 12-mm circle cover glasses (Fisher), which were placed in each well of a 24-well plate and allowed to grow for 24 h in DMEM with 10% FCS at 37 °C with 5% CO_2. Where necessary, the 12-mm circle cover glasses were coated with FN (10 μg/ml) or polylysine (10 μg/ml) overnight in PBS, respectively, before cells plating. The cells were then fixed with 4% paraformaldehyde in 0.1 M sodium phosphate (pH 7.0) for 5 min, washed three times with PBS, and permeabilized with 0.1% Triton X-PBS for 10 min before blocking with 2% bovine serum albumin with TBST (0.15 M NaCl, 1% Tris, pH 7.0, 0.05% Tween 20). Then the cells were incubated with the first antibody anti-cortactin (5 ng/μl) or anti-Fyn (Fyn3) (5 ng/μl) in 2% bovine serum albumin with TBST to stain cortactin or Fyn for 1 h. After washing three times with PBS, the cells were then incubated with fluorescein isothiocyanate-conjugated anti-mouse IgG antibody (1:40) or rhodamine-conjugated anti-rabbit IgG antibody (1:40) for 30 min. In staining actin stress fibers, the cells were incubated with rhodamine-conjugated phalloidin (1:200, 1 unit/ml) for 30 min in 2% bovine serum albumin with TBST. After the cells were washed three times with PBS, the cover glasses were mounted in a 1:1 mixture of 2.5% DABCO (Sigma) in PBS and glycerol. The cells were then visualized using a Radiance 2100 confocal microscopic system (Bio-Rad).

Cell Migration Assay—Cell motility of 3Y1-Crk fibroblasts was performed as described previously (6). Haptotactic cell migration of all the melanoma cells was analyzed using Boyden chamber cell migration assay with some modification. The conditions are described in a previous study (17). In detail, the cells were trypsinized, washed once in DMEM with 10% FCS, and washed once in serum-free DMEM. 1.5×10^5 cells were then resuspended to 560 μl of DMEM with 15 mM Hepes buffer (pH 7.2) and added to the upper well of the Boyden chamber. To investigate the effect of PP2 treatment on cell motility, the cells were added to the upper well under the same conditions in the presence of PP2 (10 μM), Me_2SO (10 μM), or PP3 (10 μM). FN (Sigma) was diluted in 1280 μl of medium as described above at a concentration of 10 μg/ml and filled the lower well of the chamber. A polyvinylpyrrolidone-free polycarbonate filter with an 8-μm pore size (Neuroprobe) was used. The chamber containing the cells was incubated for 3 h at 37 °C in a humid 5% CO_2 atmosphere. The cells at the lower surface of the filter were fixed in methanol for 30 min, washed with PBS, and then exposed to Giemsa staining for 15 s. After washing three times with PBS, the filter was mounted on a glass slide. The side of the filter to which cells had been added was scraped. The number of migrated cells was counted from photographs taken of at least eight fields at a magnification of 200× under the microscope.

Cell Spreading Assay—Cells in confluence were overnight serum-starved, harvested with 0.5% trypsin and 2 mM EDTA, and washed once with soybean trypsin inhibitor (0.5 mg/ml) in DMEM before being resuspended with DMEM at 10^5 cells/ml. The cells were then plated on dishes coated with FN (10 μg/ml) (Sigma). Photos of cells were taken at the indicated times. Single cells that were phase bright with rounded morphology were scored as nonspread, whereas those that possessed a flat shape and were phase dark were scored as spread. The percentage of spread cells was calculated by counting the spread cells in

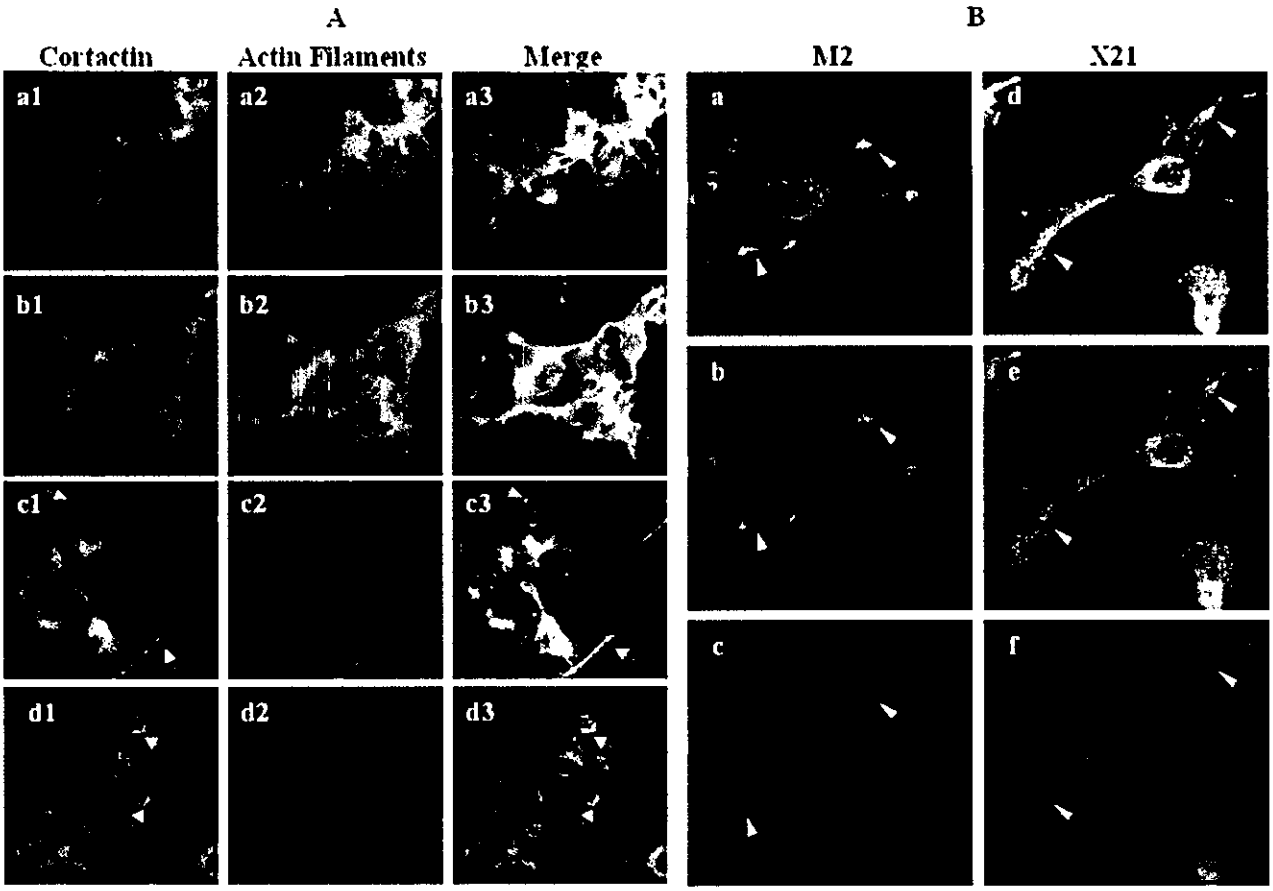

FIG. 7. **Subcellular co-localization of cortactin with actin filaments or Fyn in melanoma cells with high metastatic potential.** Co-localizations of cortactin and actin filaments (*A*) or co-localizations of cortactin and Fyn (*B*) in melanoma cell lines were investigated by immunofluorescence staining. The cells plated on 12-mm circle cover glasses were allowed to grow for 24 h in DMEM with 10% FCS at 37 °C with 5% CO_2, then fixed, permeabilized, and stained by primary antibody against cortactin (UBI) and rhodamine-conjugated phalloidin (Molecular Probes) or Fyn (Fyn3) (Santa Cruz Biotechnology) (10 ng/μl). Fluorescein isothiocyanate-conjugated anti-mouse IgG or rhodamine-conjugated anti-rabbit IgG antibody (Santa Cruz Biotechnology) were utilized as secondary antibodies. The cells were then visualized by a Radiance 2100 confocal microscopic system (Bio-Rad). *A*, co-localizations of cortactin and actin filaments in C10 (*panels a1*, *a2*, and *a3*), C19 (*panels b1*, *b2*, and *b3*), X21(*panels c1*, *c2*, and *c3*), and M2 (*panels d1*, *d2*, and *d3*). Co-localizations of cortactin and actin filaments at membrane protrusions or extensions are indicated by *arrowheads*. *B*, co-localizations of cortactin and Fyn in membrane protrusions or extensions in M2 and X21. The triangles indicate co-localizations of cortactin and Fyn. *Panels a–c*, M2; *panels d–f*, X21. *Panels a* and *d*, merged localization of cortactin and Fyn; *panels b* and *e*, anti-cortactin; *panels c* and *f*, anti-Fyn.

each microscope field. The same experiment was repeated at least three times.

Immune Complex Kinase Assay—For immune complex assay, each member of Src family kinases in cell lysates containing 500 μg of proteins was first immunoprecipitated by antibody against Fyn (UBI), Src family (Src2), Src (Src-N-16) (Santa Cruz Biotechnology), Yes, or Hck (Transduction Laboratories). Then immunoprecipitates were consequently washed using 1% Triton buffer and kinase buffer (50 mM Tris, pH 7.4, 50 mM NaCl, 10 mM $MgCl_2$, 10 mM $MnCl_2$) three times, respectively. To each sample, 1 μl of exogenous synthetic polypeptides poly-[Glu-Tyr] was added as exogenous substrate. Kinase reaction was performed in 30 μl of kinase buffer with 5 μCi of [γ-^{32}P]ATP (ICN) at room temperature for 30 min. Kinase reactions were stopped by the addition of SDS-PAGE sample buffer (2% SDS, 0.1 M Tris, pH 6.8, 10% glycerol, 0.01% bromphenol blue, 0.1 M dithiothreitol). The samples were then subjected to SDS-PAGE analysis using 8% polyacrylamide gel. The gels were then dried and exposed to autoradiography.

RESULTS

Highly Metastatic Murine Melanoma Cell Lines Exhibited Enhanced Motility and Spreading Ability on Fibronectin—To clarify differences in cell properties that correspond to the diversity of metastatic potentials of K-1735 cell lines, we measured haptotactic cell migration ability toward FN using a Boyden chamber. As shown in Fig. 1*A*, about 140 cells/field of highly metastatic cells X21 and M2 migrated through the pores of the filter in 3 h toward FN. In contrast, for low metastatic cells C19 and C10, only about 70 cells/field of C19 and no more than 10 cells/field of C10 migrated through the pores toward FN, respectively. No cell locomotion was observed in the absence of FN in any of these cell lines, suggesting that these cells exhibit FN-dependent cell motility. Cell motility under the stimulation of integrin correlates with metastatic potentials. To determine their differences in spreading abilities, time-dependent cell spreading was estimated by the percentage of flat cells in all of cells at attachment after plating on FN-coated dishes (see "Experimental Procedures"). About 70% of X21 and 45% of M2 exhibited a flat shape with multiple protrusions 30 min after plating on FN. In contrast, about 20% of C19 and 17% of C10 were spread (Fig. 1*B*). After plating on FN for 60 min, the percentages of flat cells of X21 and M2 increased to about 98%, whereas there were less than 50% C19 and C10 showing a flat shape (Fig. 1*B*). These results demonstrate that cell spreading of X21 and M2 occurs much faster than that of C10 and C19. Both cell migration and cell spreading abilities were enhanced in highly metastatic cell lines.

Analysis of Src Family Kinases Responsible for Enhanced Cell Motility of Melanoma Cells with High Metastatic Potential—Roles of Src family tyrosine kinases in cell migration of

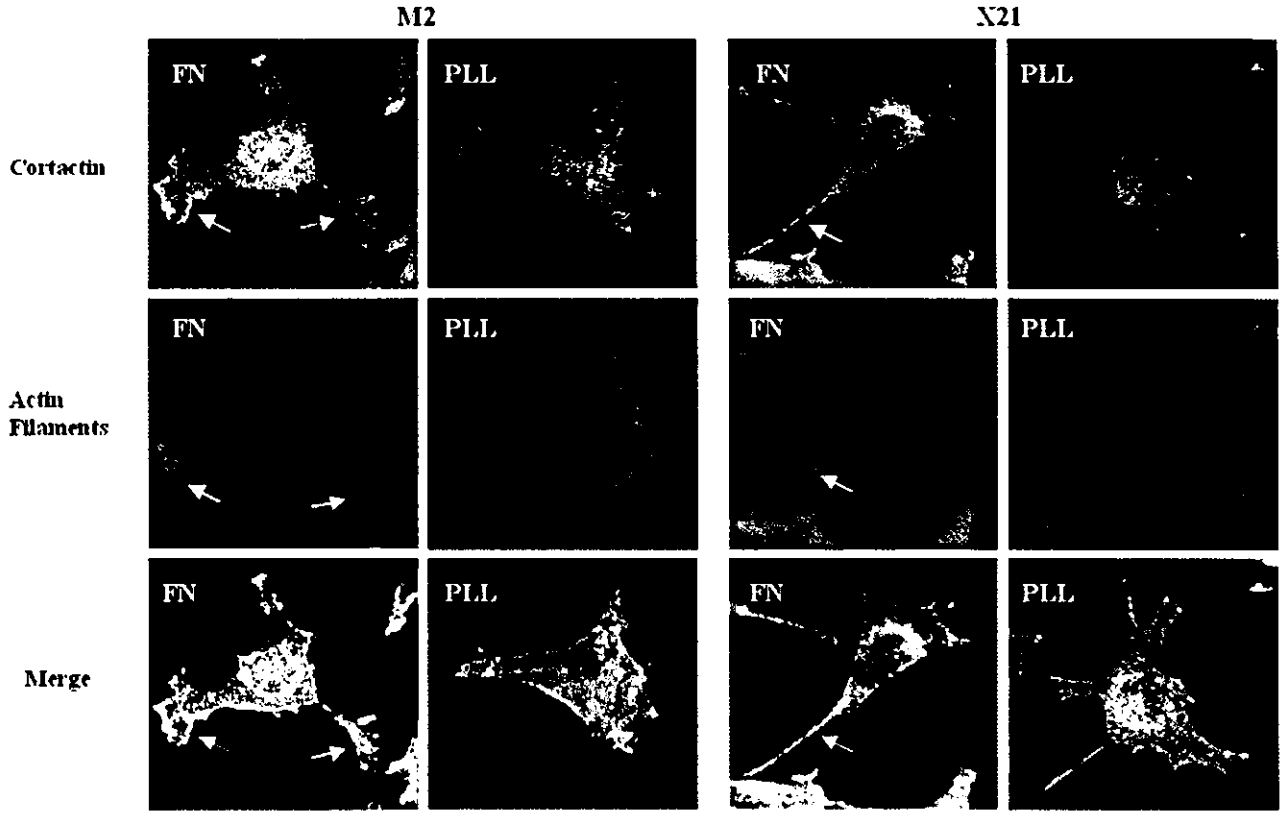

FIG. 8. **Integrin stimulated redistributions of cortactin with actin filaments in highly metastatic cells.** M2 and X21 cells were plated onto 12-mm circle cover glasses (Fisher Scientific), which were coated with FN (10 μg/ml) or polylysine (*PLL*, 10 μg/ml), overnight in PBS and allowed to grow for 24 h in DMEM with 1% FCS at 37 °C with 5% CO_2. Then co-localization of cortactin and actin filaments in highly metastatic melanoma cell lines was investigated by immunofluorescence staining using rhodamine-conjugated phalloidin (Molecular Probes) or antibody against cortactin (UBI) and fluorescein isothiocyanate-conjugated anti-mouse IgG (1:40). The cells were then visualized by a Radiance 2100 confocal microscopic system (Bio-Rad). Redistribution of cortactin co-localized with actin filaments at lamellipodias in M2 or fillopodias in X21 on FN were observed in merged images (as indicated by *arrows*).

X21 and M2 cells were investigated by the Boyden chamber in the presence of specific inhibitor of Src family kinases including Src, Fyn and Hck, PP2 (18). The inactive structural analog PP3 and Me_2SO were used as negative controls. Treatment of PP2 significantly reduced the number of cells migrating through the pores in 3 h from 140 to about 30/field (Fig. 2), whereas negative controls Me_2SO or PP3 did not show such an effect, showing that PP2 impairs cell motility of X21 and M2. These results demonstrate that some member(s) of Src family kinases play essential roles in cell migration of highly metastatic cells.

To characterize the member of the Src kinases responsible for the enhanced cell motility and spreading ability detected in highly metastatic cells M2 and X21, the kinase activities of Src, Fyn, Yes, and Hck were investigated using an *in vitro* immune complex kinase assay in the presence of exogenous synthetic polypeptides poly[Glu-Tyr] as substrates. No significant differences in kinase activities of Src and Yes were observed in any of the cell lines with different metastatic potentials (Fig. 3, *C* and *D*). In the case of Hck, the kinase activity was rather lower in X21 and M2 (Fig. 3*E*), whereas the activity of Fyn was particularly elevated in highly metastatic cells X21 and M2 compared with C10 and C19 (Fig. 3*B*). These results indicate that Fyn is a candidate Src family kinase responsible for high metastatic potential in X21 and M2 melanoma cells.

In the absence of exogenous substrate, a distinct 85-kDa protein was significantly phosphorylated by the immune complex kinase assay by pan-Src and Fyn in X21 and M2 (Fig. 3, *F* and *G*, *closed triangles*) but not in C10 or C19. This protein was not detected in protein complexes immunoprecipitated by Src (Src-N-16), Yes, or Hck (Fig. 3, *H–J*), demonstrating that this protein is specifically associated with Fyn in highly metastatic cell lines. An 80-kDa phosphorylated band was also immunoprecipitated by Src, Hck, or Yes only in M2 (Fig. 3, *H–J*, *open triangles*). Judging from differences in molecular size and substrate specificity, this protein is distinct from the 85-kDa protein observed in both X21 and M2.

Overexpressed and Hyperphosphorylated Cortactin Was Specifically Associated with Fyn in Highly Metastatic Cells—Cortactin, a protein of 80/85 kDa, acts as a potential linker between membrane-located receptors and cytoskeleton, primarily affecting cell motility and invasion (11–13). Because the molecular size of cortactin appeared close to the size of the protein associated with Fyn in X21 and M2 (Fig. 3*G*), we examined the expression and tyrosine phosphorylation of cortactin in these murine melanoma cells. As expected, tyrosine phosphorylation of cortactin was significantly elevated in X21 and M2 (Fig. 4*A*, *lanes 2* and *4*) compared with that of C10 and C19 (Fig. 4*A*, *lanes 1* and *3*). Expression levels of cortactin in X21 and M2 were also up-regulated (Fig. 4*B*, *lanes 1* and *3*). Tyrosine phosphorylation levels of cortactin were much reduced by Src family kinase inhibitor PP2 in X21 and M2 in contrast to PP3 (Fig. 4*C*), confirming that Src family kinases are responsible for tyrosine phosphorylation of cortactin in X21 and M2. At the same time, we investigated the expression and tyrosine phosphorylation of other substrates of Src family kinases such as $p130^{Cas}$, FAK, and paxillin. As shown in Fig. 4*B*, tyrosine phosphorylation of $p130^{Cas}$ was reduced in X21 and M2 compared with that in C10 and C19, and no significant differences

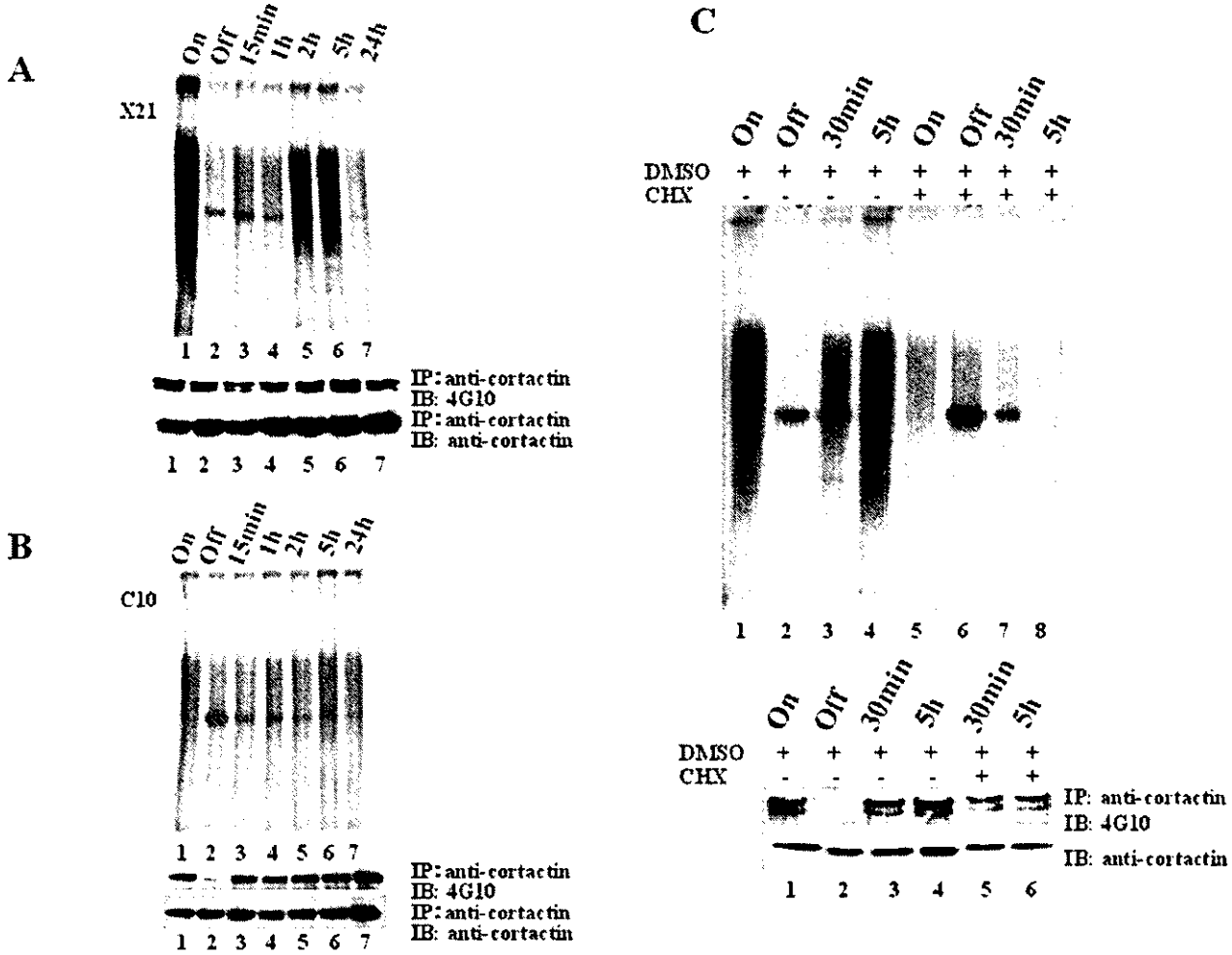

FIG. 9. **Late phase activation of Fyn under integrin stimulation in cells with high metastatic potential.** The cells were either serum-starved (on dish), held in suspension for 30 min (off dish), or plated onto FN-coated dishes for the times indicated. Fyn in equal portions of cell lysates were isolated by immunoprecipitation (*IP*) using antibodies against Fyn (UBI), and the immunoprecipitates were labeled by [γ-^{32}P]ATP in an *in vitro* kinase assay in the presence of exogenous synthetic polypeptides poly[Glu-Tyr]. The labeled proteins were analyzed by SDS-PAGE and visualized by autoradiography. Tyrosine phosphorylation of cortactin in equal cell lysates were also analyzed by immunoprecipitation using antibody against cortactin and immunoblotting (*IB*) by tyrosine phosphorylation antibody 4G10. The results presented here are representative of experiments performed at least twice. *A*, integrin-stimulated Fyn activation (*upper panel*) and tyrosine phosphorylation of cortactin (*lower panel*) exhibited a peak at 2–5 h after plating in X21. *B*, no peak of Fyn activation and tyrosine phosphorylation of cortactin under integrin stimulation in C10 was observed. *C*, effects of cycloheximide on integrin-induced activation of Fyn (*upper panel*) and tyrosine phosphorylation of cortactin (*lower panel*). The cells were either serum-starved, held in suspension for 30 min, or plated onto FN-coated dishes for the times indicated in the absence (*lanes 1–4*) or presence (*upper panel, lanes 5–8*; *lower panel, lanes 5* and *6*) of cycloheximide (10 μg/ml) (Sigma). Then *in vitro* kinases assay was carried out in the presence of poly[Glu-Tyr] as described above.

of FAK tyrosine phosphorylation were detected among these cells. Tyrosine phosphorylation and expression of paxillin in C10 were much lower, but they were at the same level in C19 as in X21 and M2. Cortactin was the only phosphotyrosine-containing protein showing significantly elevated phosphorylation levels in highly metastatic cell lines.

Further study confirmed that cortactin was specifically associated with Fyn in X21 and M2. It was observed that the amount of cortactin coupling with Fyn in X21 and M2 was significantly greater than that in C10 and C19 (Fig. 5*A*). Correspondingly, tyrosine phosphorylation of the protein with a size of 85 kDa associated with Fyn in X21 and M2 was also observed (Fig. 5*B*, *lanes 2* and *4*). In contrast, an 80-kDa tyrosine-phosphorylated protein associated with Src was only observed in M2 but not in X21 (Fig. 5*C*, *lane 4*). This M2-specific protein was later identified as a *gag* protein derived from murine mammary tumor virus by means of mass spectrometry analysis,[2] which might be infected during the establishment of the M2 cell line by *in vivo* selection. There has been no report on tyrosine phosphorylation of this protein so far, and its roles on the metastatic potential of M2 are currently under investigation.

To provide additional evidence for essential roles of kinase-substrate cooperation between Fyn and cortactin, v-Crk transformed 3Y1 fibroblasts were used in which Fyn was reported to be activated by v-Crk (19). Following Fyn activation, elevated cell motility was observed in 3Y1-Crk cells compared with mock-transfected 3Y1-vec cells as shown in Fig. 6*A*. At the same time, tyrosine phosphorylation of cortactin was significantly enhanced in 3Y1-Crk fibroblasts (Fig. 6*C*), and the same molecular sizes of phosphoproteins were obvious among Fyn-associated phosphoproteins apart from p130^{Cas}, which has

[2] J. Huang, T. Asawa, T. Takato, and R. Sakai, unpublished data.

been reported to be associated with Fyn (Fig. 6*B*). These results in fibroblasts also support the possibility that cortactin tyrosine phosphorylation is regulated by Fyn in relation to signaling of cell migration.

Subcellular Localization of Fyn and Cortactin in Melanoma Cell Lines—Because cortactin has been functionally identified as an actin-associated protein (20–22), we also investigated co-localizations of cortactin with actin in C10, C19, X21, and M2. First, different distribution patterns of actin filaments between low and highly metastatic cells were noticed on non-coated glass slides. Significantly increased amounts of actin filaments were found at cell membrane protrusions in highly metastatic cells X21 and M2 (Fig. 7*A*, *panels c2* and *d2*). In contrast, actin filaments were widely (nonspecifically) observed in cell matrix in C10 and C19 (Fig. 7*A*, *panels a2* and *b2*). It was also observed that overexpressed cortactin was localized in these cell membrane protrusions specific to X21 and M2 (Fig. 7*A*, *panels c1*, *d1*, *c3*, and *d3*), implying that cortactin is associated with signaling of actin cytoskeleton organization near the membrane in highly metastatic cells. Results of staining of Fyn and cortactin demonstrated that most of cortactin and Fyn were distributed at cell membrane protrusions in M2 and X21 (Fig. 7*B*, *panels a* and *d*, *arrows*), showing apparent co-localization of cortactin and Fyn at these structures.

To further investigate the role of cortactin in highly metastatic cells, we explored co-localization of cortactin with actin filaments in X21 and M2 under the stimulation of integrin. As shown in Fig. 8, cortactin was co-localized with actin filaments at lamellipodias or fillopodias in M2 or X21, which were formed under the stimulation of FN.

Late Response of Fyn Activation by FN Requires de Novo Protein Synthesis—To illustrate molecular mechanisms underlying FN-stimulated redistribution of cortactin and formation of lamellipodia or fillopodia in highly metastatic cells X21 and M2, we explored the activity of Fyn under FN stimulation by *in vitro* kinase assay with poly[Glu-Tyr]. In X21, Fyn activity was relatively high when cells were at attachment (Fig. 9*A*, *lane 1*), whereas it was sharply reduced when cells were detached and kept in suspension for 30 min (Fig. 9*A*, *lane 2*). The activity of Fyn was restored 2 or 5 h after cells were plated on FN (Fig. 9*A*, *lanes 5* and *6*). Corresponding to the activation of Fyn, tyrosine phosphorylation of cortactin also exhibited a similar time course (Fig. 9*A*, *lower panel*). A similar pattern of activation of Fyn and tyrosine phosphorylation of cortactin by FN was also observed in M2.[2] In contrast, levels of Fyn activity were not significantly changed in C10 and C19 after each indicated time plated on FN (Fig. 9*B*).[2] Although tyrosine phosphorylation of cortactin was abolished by detachment, no obvious peaks in tyrosine phosphorylation of cortactin after each indicated time plated on FN were observed in these cells (Fig. 9*B*, *lower panel*). Preceding elevated Fyn activity at 2–5 h after stimulation, the expression level of cortactin was also increased from 1 to 2 h in X21 (Fig. 9*A*, *lower panel*). The same results were observed in M2.[2]

The late phase activation of Fyn demonstrated by both M2 and X21 on FN raised the possibility of yet unidentified regulatory mechanisms in integrin-mediated Fyn activation. To determine whether *de novo* synthesis of regulatory proteins in this process is required, we investigated Fyn activity in the presence of cycloheximide (CHX), a protein synthesis inhibitor. As expected, elevated expression of cortactin induced by integrin stimulation was antagonized by CHX at 5 h after plating (Fig. 9*C*, *lower panel*, *lane 6*). At the same time, it was observed that activation of Fyn was significantly blocked by the treatment of CHX at 5 h after plating (Fig. 9*C*, *upper panel*, *lane 8*) compared with the control (Fig. 9*C*, *upper panel*, *lane 4*). Tyrosine phosphorylation of cortactin was also down-regulated by CHX treatment (Fig. 9*C*, *lower panel*, *lane 6*). The same results were observed in M2.[2] These findings indicate that *de novo* protein synthesis is involved in the late phase activation of Fyn by FN stimulation.7

DISCUSSION

Previous studies have shown that Fyn is an essential regulator in integrin-mediated processes including actin cytoskeleton organization, cell migration, and adhesion in normal cells (23–25). A recent study also demonstrated that Fyn is prerequisite for normal keratinocyte migration and squamous carcinoma invasion (26). However, little is known regarding the functional roles of Fyn in tumor metastasis. In this study, in contrast to Src, Yes, and Hck, enhanced levels of Fyn activity and late phase activations of Fyn after stimulation by FN were observed in highly metastatic murine melanoma cell lines. Activated Fyn caused hyperphosphorylation of cortactin and formation of stable complex between Fyn and cortactin in these metastatic cell lines, indicating that Fyn and cortactin are key molecules in the integrin signaling pathway during the development of cancer metastasis.

Activation of Fyn by integrin signaling is mediated by many kinds of proteins involved in integrin signaling, which includes caveolin 1, tyrosine kinases, FAK, or receptor protein tyrosine phosphatase α (23, 25, 27). It has been observed in several studies that the activity of Src is enhanced 20–40 min following FN stimulation in NIH 3T3 fibroblasts (28–31). In this study, it was observed that Fyn activation occurs as late as 2–5 h after fibronectin stimulation in metastatic melanoma cell lines, and integrin-mediated activation of Fyn requires *de novo* protein synthesis. One possibility is that the up-regulation of cortactin that occurred approximately 1–2 h after stimulation is a primary event that triggers the activation of Fyn and phosphorylation of cortactin itself. As a special substrate associated with Fyn in metastatic cells, it is possible that cortactin regulates the activity of Fyn through physical associations to SH2 of Fyn. Another possibility is that a third molecule(s), which is specifically expressed in metastatic cell lines under stimulation of integrin, might regulate activation of Fyn, although this protein(s) has not been identified. In this paper, we do not demonstrate that cortactin is a direct substrate of Fyn kinase. According to a recent paper, tyrosine phosphorylation of cortactin occurs via activation of Rac1 by c-Src in C3H fibroblasts (38). Therefore, there is a possibility that cortactin phosphorylation by Fyn is regulated in a similar indirect manner in highly metastatic melanoma cell lines.

Cortactin was first identified as a p80/85-kDa v-Src substrate in chicken embryo cells transformed by v-Src oncogene (32). It was implicated in the progression of breast tumors through gene amplification at chromosome 11q13 (33). The importance of tyrosine phosphorylation of cortactin in metastasis was also implicated in a recent report (34). In this study, overexpression and enhanced tyrosine phosphorylation of cortactin in highly metastatic cells was observed, and it was also clarified that cortactin was specifically associated with Fyn in cells with high metastatic potential. When the activity of Fyn was inhibited by PP2, tyrosine phosphorylation of cortactin was also down-regulated. Moreover, corresponding to up-regulated membrane redistribution of cortactin, co-localized cortactin and Fyn at cell membrane protrusions in highly metastatic cells were also observed. Taken together, these results indicate that cortactin is associated with Fyn in integrin-mediated signaling processes in cancer metastasis. Previous reports have shown that cortactin is primarily localized within peripheral cell structures such as lamellipodia, pseudopodia, and membrane ruffles and has been suggested to operate as a potential